# NOISE REDUCTION TECHNIQUES FOR PARTIAL DISCHARGE CLASSIFICATION IN XLPE CABLE JOINT

**NORATIKA BINTI MOHD ZIN**
**KMA150015**

**FACULTY OF ENGINEERING**
**UNIVERSITY OF MALAYA**
**KUALA LUMPUR**

**2017**

# NOISE REDUCTION TECHNIQUES FOR PARTIAL DISCHARGE CLASSIFICATION IN XLPE CABLE JOINT

**NORATIKA BINTI MOHD ZIN**
**KMA150015**

**DISSERTATION SUBMITTED IN FULFILMENT OF THE REQUIREMENTS FOR MASTER OF ENGINEERING (POWER SYSTEM)**

**FACULTY OF ENGINEERING**
**UNIVERSITY OF MALAYA**
**KUALA LUMPUR**

**2017**

**UNIVERSITI MALAYA**

**ORIGINAL LITERARY WORK DECLARATION**

Name of Candidate: NORATIKA BINTI MOHD ZIN

Registration/Matric No: KMA150015

Name of Degree: Master of Engineering (Power System)

Title of Thesis ("this Work"): NOISE REDUCTION TECHNIQUES FOR PARTIAL DISCHARGE CLASSIFICATION IN XLPE CABLE JOINT

Field of Study: High Voltage Engineering

I do solemnly and sincerely declare that:

1. I am the sole author/writer of "this work";
2. This work is original;
3. Any use of any work in which copyright exists was done by way of fair dealing and for permitted purposes and any excerpt or extract from, or reference to or reproduction of any copyright work has been disclosed expressly and sufficiently and the title of the Work and its authorship have been acknowledged in this Work;
4. I do not have any actual knowledge nor do I ought reasonably to know that the making of this work constitutes an infringement of any copyright work;
5. I hereby assign all and every rights in the copyright to this Work to the University of Malaya ("UM"), who henceforth shall be owner of the copyright in this Work and that any reproduction or use in any form or by any means whatsoever is prohibited without the written consent of UM having been first had and obtained;
6. I am fully aware that if in the course of making this Work I have infringed any copyright whether intentionally or otherwise, I may be subject to legal action or any other action as may be determined by UM.

Candidate's Signature Date

Subscribed and solemnly declared before,

Witness's Signature Date

Name:

Designation:

## ABSTRACT

Cable joints of cross-linked polyethylene (XLPE) are the weakest point in a power system and can cause insulation failures with the present of partial discharge (PD). Therefore, it is important to monitor PDs at cable joints and determine the type of the defect that exists at cable joints. Determination of the type of the defect at cable joints can reduce the repair time and maintenance cost. In this project, defect type in cable joint determination using partial discharge testing under noisy condition was carried out. Five joints of cross-linked polyethylene cable including artificial defects were created according to the conditions usually found at site. Various noise reduction techniques were applied to denoise the PD signals and the denoised PD signals were used to determine different types of defect in cable joints. The input features from different noise reduction techniques were applied to train the classifier to determine the type of the problem in the samples. Determination of the defect type was performed using Support Vector Machine (SVM) after DFT, WPT and DWT techniques. The results were compared between each noise reduction methods to evaluate the performance of the applied methods. It was found that the noise reduction technique on partial discharge signals from cable joint defects using discrete Fourier transform (DFT) yields a better accuracy than wavelet packet transform (WPT) and discrete wavelet transform (DWT).



**Keywords:** Partial discharge measurement, support vector machine, high voltage engineering, cable insulation, signal processing

## ABSTRAK

Sambungan kabel polietilena silang (XLPE) adalah titik paling lemah dalam sistem kuasa dan boleh menyebabkan kegagalan penebat dengan masa pelepasan separa (PD). Oleh itu, adalah penting untuk memantau PD pada sendi kabel dan menentukan jenis kecacatan yang wujud pada sambungan kabel. Penentuan jenis kecacatan pada sambungan kabel boleh mengurangkan masa pembaikan dan kos penyelenggaraan. Dalam kerja ini, penentuan jenis kecacatan pada kabel menggunakan pengukuran pelepasan separa di bawah persekitaran yang bising telah dilakukan. Lima sambungan kabel polietilena (XLPE) dengan kecacatan yang dibuat secara buatan telah disediakan berdasarkan kecacatan yang sering ditemui di tapak. Teknik pengurangan hingar yang berbeza digunakan untuk mengecam isyarat PD dan isyarat PD denoised digunakan untuk menentukan jenis kecacatan yang berlainan dalam sambungan kabel. Ciri-ciri input dari teknik pengurangan hingar yang berbeza digunakan untuk melatih pengelas untuk mengklasifikasikan setiap jenis kecacatan dalam sampel bersama kabel. Penentuan jenis kecacatan dilakukan menggunakan Mesin Vektor Sokongan (SVM) yang mempunyai teknik-teknik seperti DFT, WPT dan DWT. Hasilnya dibandingkan antara setiap kaedah pengurangan hingar untuk menilai prestasi teknik yang digunakan. Telah didapati penentuan teknik pengurangan hingar ke atas isyarat pelepasan separa menggunakan transformasi Fourier diskret (DFT) menghasilkan ketepatan yang lebih baik berbanding transformasi paket wevlet (WPT) dan transformasi wevlet diskret (DWT).

## ACKNOWLEDGEMENT

Firstly, all my thanks go to the Almighty Allah for the blessing for me in completing this research work at a crucial time. I wish to express my sincerest thanks to my supervisor, Associate Professor Ir. Dr. Hazlee Azil Illias for all his valuable support and guidance. His expertise in high voltage engineering has helped me in my research and finishing this work.

I wish my deepest gratitude to my families for their prayers, continuous encouragement and support, which gives me inspiration to finish my research. Finally, I thank my husband for being supportive and fully understanding me throughout my study.

# TABLE OF CONTENTS

# LIST OF FIGURES

## LIST OF TABLES

## LIST OF ABBREVIATIONS

| | |
|---|---|
| **AC** | Alternating Current |
| **DWT** | Discrete Wavelet Transform |
| **DFT** | Discrete Fourier Transform |
| **DTFT** | Discrete-Time Fourier Transform |
| **FFT** | Fast Fourier Transform |
| **HPF** | High Past Filter |
| **HV** | High Voltage |
| **LDPE** | Low Density Polyethylene |
| **LPF** | Low Past Filter |
| **pC** | Pico Columb |
| **PD** | Partial Discharge |
| **QMF** | Quadrature Mirror Filter |
| **ROI** | Region of Interest |
| **SVM** | Support Vector Machine |
| **WPT** | Wavelet Packet Transform |
| **WP** | Wavelet Packet |
| **WT** | Wavelet Transform |

# CHAPTER 1: INTRODUCTION

## 1.1 Introduction

As defined by IEC 60270 standard, partial discharge (PD) is a localized discharge of electrical, which only bridges partially the insulation between 2 conductors [1]. PD is the electrical stress concentration on the surface or in the insulation. There are electrical sparks occur within the insulation of medium and high voltage electrical equipment that can cause damage. It is due to high voltage applied to an insulation is higher than the inception of discharge voltage. When the electrical field stress becomes very high, a PD occurs. This causes electrical failure and insulation to break down. The National Electrical Code (NEC) implies that PD are the first sign of insulation deterioration. Cables, transformers and switchgear experience the greatest failures from insulation breakdown. PD will lead to degradation and breakdown of insulation.

It is very important to monitor the insulation condition level because if there is a failure happens in any parts of a power system, it can cause damage to the equipment. Cable joints of XLPE cable are weak dielectrically points, which can cause discontinuity of insulation. PD can decrease the life of high voltage equipment because of insulation damage. Since PD can cause disastrous results to safety and financial, identifying PD events is a key indicator in condition monitoring of the insulation [2]. Therefore, it is crucial to detect PD at its early stage to replace the faulty parts as soon as possible at the correct time. PD types include void in solid insulation, void in liquid, electrical tree around a sharp point, electrical floating potential, surface discharge and corona.

PD is caused by discontinuities and flaws in high voltage electrical insulation and if left undetected, it can eventually lead to the full breakdown of the insulation system. The insulation defect is considered as a weak point for PD to occur. It normally happens because of defect such as delamination of power cable and insulation material, crack or air bubbles. Many PD determination works were performed in laboratories under no noise. However, in actual sites, PD measurement has low detection sensitivity due to the external noise interference [3]. PD does not cause immediate breakdown since it is only occur within the defect of insulation. However, it will affect the performance in a long run because of degradation of insulation. This is due to the development of PD may cause system breakdown at certain conditions. It depends on the type of the defect, location and quality of an insulation.

## 1.2 Problem statement

Many research works have been done on denoising of PD signals and it has been better and better. However, a perfect denoising method has not been achieved yet. Most previous research works used artificial noise generated by including random noise with different mean and standard deviation instead of actual noise encountered on site. Hence, another research is essential on how various noise levels and signal denoising techniques affect classification accuracy.

## 1.3 Objectives of research

The objectives of this research are:

1. To perform measurement of partial discharge (PD) from artificially prepared cable joint defects.

2. To apply different noise reduction methods for partial discharge classification in XLPE cable joint.
3. To compare the performance between each noise reduction method and the previous work.

## 1.4 Dissertation Structure

This report consists of five chapters. In Chapter 1, the introduction of PD phenomenon, problem statement of the research work and objectives of the research are explained. In Chapter 2, literature review about PD phenomena, detection method of PD and review on previous research works on classification using SVM, DFT, WPT and DWT is also included. In Chapter 3, the methodology of the work is described in details on each analysis techniques. The preparation of the test samples and the experiment setup of five different PD defects types are explained. Chapter 4 reports on the results that have been obtained from this work and also comparison with the existing works. Finally, Chapter 5 is about the conclusions of the work and future work that can be performed.

# CHAPTER 2: PARTIAL DISCHARGE PHENOMENON

## 2.1 Partial Discharge

The life span of high voltage power cables is dependent on its insulation quality especially for insulated switchgear and transformer. PD is crucial to be detected at early stage to avoid the system damage. PD testing must be done once fault has been detected at a very early stage and PD pattern needs to be obtained to recognise and determine the risk of insulation breakdown. Testing will indicate if the existing component needs a service or replacement [1].

## 2.2 Partial Discharge Equivalent Circuit

As suggested by IEC 60270 standard, Figure 2.1 shows an equivalent circuit of PD measurement. Through the test, the presence of PD and its location in electrical equipment can be detected. Assuming a piece of an equipment with a tiny air void in the insulation due to constant degradation and the void was exposed to PD [2].

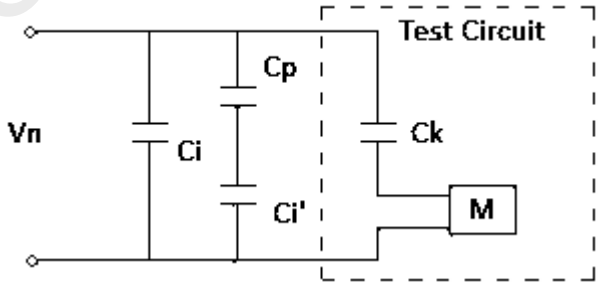


Figure 2.1: Equivalent circuit of a PD test

The circuit components are:

Ck = capacitance of the coupling capacitor

Ci' = capacitance of the remaining insulation around the air void

Cp = capacitance of the void in the insulation due to defect

Ci = capacitance of the insulation system

Vn = voltage applied

M = measuring system in series

At certain inception voltage, partial discharge occurs because of the electric field becomes stronger to bridge the air void (Ci) in the insulation. The voltage, Vn around charge across Ci increases after the air gap breakdown. The parallel capacitances provide extra charges around Ck and Ci or the applied voltage. Ck and Ci discharge a short pulse into Ci' to supply excessive charges. However, it decreases the voltage across all capacitances and Vn reacts by charging all capacitances in the system back to Vn.

PD test is performed by measuring directly the pulse discharged into Ci' through the coupling capacitor Ck. In the circuit, the system is represented by a single box but in actual, it includes the measuring device, connecting cables and coupling device.

There are a lot of types of PD such as internal PD, surface PD and corona PD. The insulator used in high voltage (HV) system is not fully perfect because there are presence of bubbles and impurities. The insulation degrades in long term and will allow PD to occur. PD is caused by multiples reasons and it will always become worse until it leads to flashover, which occurs at a peak voltage. It is due to the field strength in excess of insulation withstand capability. The overall insulation system remains capable of withstanding the applied electric field, except the defect site where PDs occur. Figure 2.2 shows an insulation withstand capability against applied field.

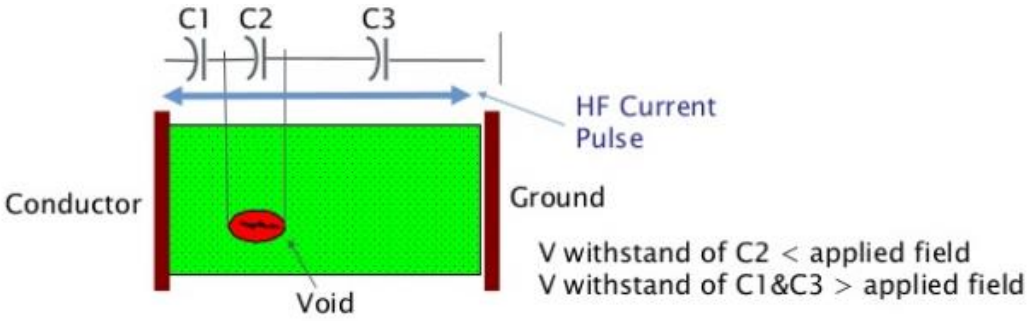


Figure 2.2: Insulation withstand capability against applied field

## 2.3 Types of PD

There are many types of PD such as surface discharges, corona discharges and internal discharges.

### 2.3.1 Internal PD

This type of PD occurs in defects, voids or cavities within the solid insulation as shown in Figure 2.3, which appear as cracks, delamination and air bubbles due to manufacturing processes or in power cable accessories. It can occur in all types of insulation including oil and gas. When PD activity is repetitive, it causes degradation of insulation material and eventually leads to breakdown.

Figure 2.3: Internal PD

### 2.3.2 Surface PD

Surface discharge happens in the insulation surface, causing treeing and tracking as shown in Figure 2.4. This type of PD causes insulation degradation on the surface of solid insulation. It is due to defects along the insulation surface under high field stress. This leads to ionization of air around the insulation or impurities, which causes it to become conductive.

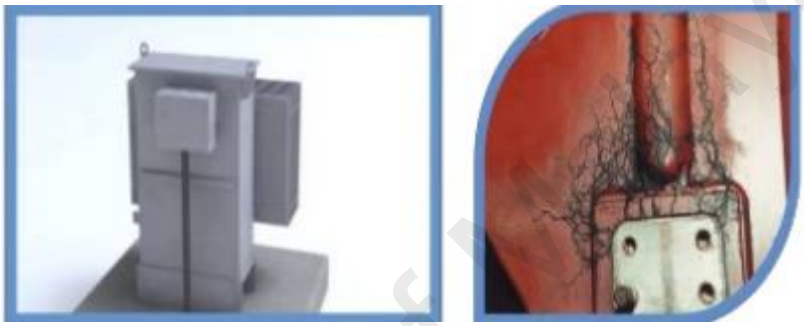

Figure 2.4: Surface discharges causes tree and track

### 2.3.3 Corona PD

Corona discharges occur in gaseous dielectrics in the present of in homogenous field. It happens due to the ionisation of air between high voltage electrode and the ground or at sharp point under high voltage as shown in Figure 2.5.

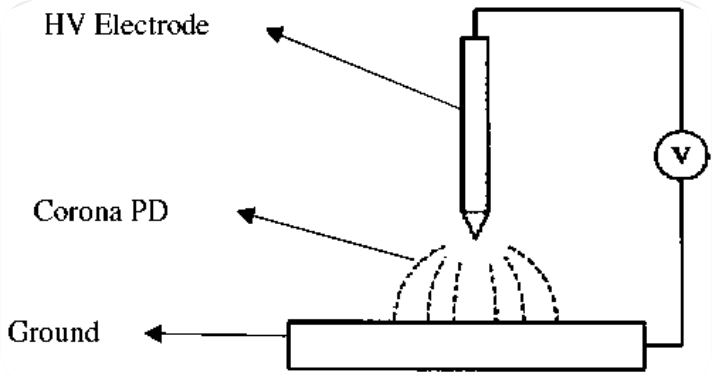


Figure 2.5: Corona PD

## 2.4 Statistical Features

PD data can be categorized into 2, which are pulse distributions and pulse height distributions. The pulse distributions are the number of PDs versus the phase angle while for the pulse height distributions are the PD charge magnitude versus phase angle. Statistical features from PD distributions are skewness, kurtosis, variance, mean and parameter of Weilbull [4].

The statistical data are calculated by:

$$\text{Mean} : \mu = \frac{\sum_{i=1}^{N} x_i f(x_i)}{\sum_{i=1}^{N} f(x_i)} \tag{2.1}$$

$$\text{Variance} : \sigma^2 = \frac{\sum_{i=1}^{N} (x_i - \mu)^2 f(x_i)}{\sum_{i=1}^{N} f(x_i)} \tag{2.2}$$

$$\text{Skewness} : S_k = \frac{\sum_{i=1}^{N} (x_i - \mu)^3 f(x_i)}{\sigma^3 \sum_{i=1}^{N} f(x_i)} \tag{2.3}$$

$$\text{Kurtosis} : K_u = \frac{\sum_{i=1}^{N} (x_i - \mu)^4 f(x_i)}{\sigma^4 \sum_{i=1}^{N} f(x_i)} - 3 \tag{2.4}$$

where:

$x_i$ is distribution discrete values,

$f(x_i)$ is the function,

$N$ is the data size.

The PD pulse rate probability distribution is expressed by the Weibull function [5, 6] using

$$F(q;\alpha;\beta) = 1 - \exp\left[-\left(\frac{q}{\alpha}\right)^{\beta}\right] \quad (2.5)$$

where $\alpha$ and $\beta$ represent every pulse height graph and PD pulse magnitude is denoted by $q$.

The features of $\alpha$-, $\beta$-, $\alpha$+ and $\beta$+ are extracted from the positive and negative pulse height [7]. The pulse height graph is determined by the Weibull for statistical analysis while maintaining relevant data. These values can be used as the input for classifiers with mean, kurtosis, variance and skewness. The objective of the extracting features is to obtain useful input data from the raw PD data to show the PD pattern of a specific defect [8].

## 2.5 Classification features of PD

In this work, there are few classification techniques for PD in order to have a better representative, which is called as feature extraction. These features can be obtained from the analysis techniques to utilize as an input for classification process. The features are support vector machine, discrete wavelet transform, discrete Fourier transform and wavelet packet transform.

### 2.5.1 Support Vector Machine (SVM)

SVM has been used widely as a classifier for the type and source of PD. It has drawn more attention in diagnostics and prediction due to its better generalization ability, effective classification and superior performance in cases of having a small data for training [9]. It is a learning technique, which is based on creating boundary separation between two groups of data set [10]. SVM is a machine that uses the main

of SVM concept, which is Kernel. Using this method, SVM can be adjusted to many tasks using kernel functions and various algorithms.

SVM works in pattern recognition matters including nonlinear, tiny sample size and huge dimensionality [11]. The classification using SVM requires a pre-processing of the input for different PD sources, obtained by phase resolved partial discharge pattern. The data was separated into some phase distributions and the lowest magnitude, highest magnitude and the number of PD were determined [12].

For example, a data set $X$ is composed by samples $x_i$, $i = 1, \ldots, N$, each of them defined by $n$ features and belonging to a known class $y_i$. Then, each sample is knows as a vector in an $n$-dimension of input space. According to the training data, a separated surface with the largest margin between each class can be obtained and the shape is suitable to fit the data distribution with good generalisation when tested with untrained data. Figure 2.6 shows input space in two-dimensional with a data separated in 2 classes. The data is separated by some planes but only one of them maximizes the margin. This is known as the *optimal hyperplane* pursued by SVM.

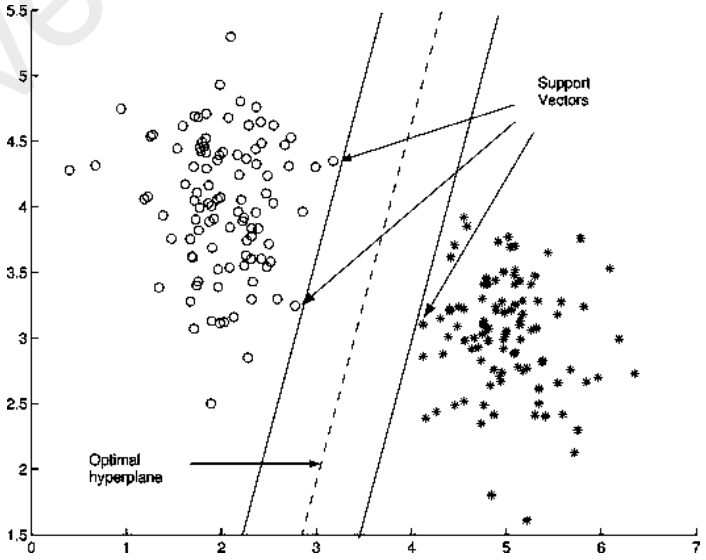


Figure 2.6: Sample of two sets by SVM

To find the optimum hyperplane, SVM search automatically the training data subset, called *support vectors* that lie in the boundaries of class. The separated surface is gained by data mapping into *feature space* followed by the development of a hyper-plane of linear. When it is re-mapped into the space of input, it results in a complex non-linear separation surface to segregate the data. The outcome was obtained by quadratic optimisation problem [13]. The frequency spectrum has stronger feature in identifying PD sources than time features while Radial Basis Function (RBF) kernel function gives better recognition rate than other kernels function,

$$\min_{w,b,\xi}\left(\frac{1}{2}\cdot\overrightarrow{w^T}\cdot\overrightarrow{w}+C\cdot\sum_{i-1}^{N}\xi_i\right) \tag{2.6}$$

subject to:

$$\begin{aligned}&\overrightarrow{w}-\sum_{i-1}^{N}\alpha_i y_i\varphi(x_i)\\&y_i[\overrightarrow{w^T}\cdot\overrightarrow{\varphi}(x)+b]=y_i\left[\sum_{i=1}^{N}\alpha_i y_i\overrightarrow{\varphi}^T(x_i)\overrightarrow{\varphi}(x)+b\right]\geq 1-\xi_i,\\&\xi_i\geq 0,\end{aligned} \tag{2.7}$$

where $x_i$ is input vector of $i$, $y_i$ is the assigned class, $N$ is the training set size, $w$ is the weight vector, $b$ is a bias, $\xi_i$ is a separation of data point $i$, $\varphi(x)$ is the mapping function set, $C$ is a cost and $\alpha_i$ is a Lagrange multiplier. SVM was implemented in recognition of PD sources through PD signals obtained experimentally in time and frequency domains [14]. The distribution features, such as Weibull skewness factor, Weibull shape factor beta, normalized quantity number (NQN), skewness and kurtosis of the PD pulse distributions were used as the input data for SVM [15].

The kernel transformation function fails to fully separate the data, a slack error variable is used to create a margin decision function to do the data separation [16]. The linear optimal plane is constructed by the process of decision function through

dimensional space, called a hyperplane. The linear function defines the hyperplane with two parameters *w* and *b* [17].

### 2.5.2 Discrete wavelet transform (DWT)

DWT was used to extract PD signals from 11 kV underground cable [18]. It was shown that wavelet transform (WT) is applicable to extract PD signals from the worst noisy condition but it is more complex compared to Fourier transform (FT) due to requiring expertise. The selection of the best mother wavelet was done for auto-determining the threshold by implementing WT to PD signal denoising. DWT was also applied to differentiate the acoustic PD signals [19].

An better method for DWT application with denoising to PD signals was proposed in [20]. First, the work defined the DWT filter structure. Then, analysis of the frequency bands was done on the wavelet coefficients in energy distribution and approximations in PD signals. Lastly, a DWT-based denoising technique was proposed and validated. They are approximations, which belong to the low frequency and detail for high frequency.

This method was used to decompose the signals of PD with the different sub-band signals. Through the decomposed signals, the real shape signals of PD were estimated. Thus, it was successfully eliminating noise from the PD signals. The real shape of PD signals, which is obtained using DWT technique can be used in the classification of PD [18]. DWT was applied to extract relative features from different PD patterns according to different types of PD [21]. DWT is a process of filtering and down sampling signal and decomposes it into two coefficients with respect to the frequency components. They are approximations, which belong to the low frequency and detail for high frequency [22].

DWT procedure from CWT by replacing *p=p0m* and *q= q0p0m*. DWT of a discrete signal x[n] is calculated using

$$DWT(p,q) = \frac{1}{\sqrt{p_o^m}} \sum_n x[n] g\left[\frac{q - nq_0 p_o^m}{p_o^m}\right] \quad (2.8)$$

where:

*g* represents for mother wavelet;

*n* represents as integer where sample taken and;

*p* and *q* are a discrete manner.

Quadrature mirror filter (QMF) that contains high pass filter h[n] and low pass filter I[n] are mirror phase of each other. For instance, signal x[n] got in both of HPF and LPF. To obtain the coefficients of dwt, the output from the filters need to down again by a factor of 2. Next, the output of HPF secured when down sampling done and after that the approximate coefficients which is from LPF gain details. Then, again the approximate coefficients are given to HPF and LPF while the process becomes continued and repeated. Both of the filters related by [23]

$$h[L-1-n] = (-1)^n l[n] \quad (2.9)$$

Both filters are related by the *L* equation which represents the filter length, known as QMF. Figures 2.7 and 2.8 show the DWT decomposition levels and reconstruction levels where the process continued when coefficients are given to both filters.

Denoising type method of DWT results in the coefficient of DWT for signal that also includes DWT thresholding. There are two types of thresholdings, which are soft and hard thresholding. In order to recover the coefficients signal, the multi-resolution signal decomposition feature is used to eliminate other sources. Next, some parameters are made to ensure that the wavelet process can happen for denoising of

the PD signals, for example mother wavelet selection, decomposition level choice, thresholding function selection. Wavelet transform is a signal analysis that can give a good alternative description of the signal representation [24].

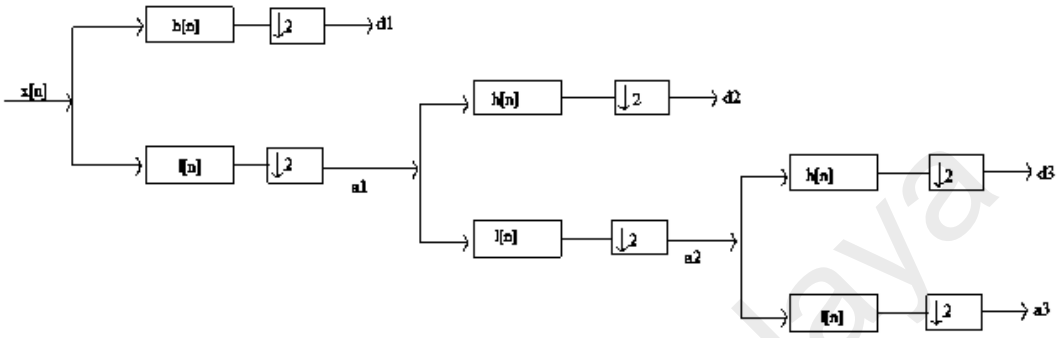


Figure 2.7: DWT decomposition levels

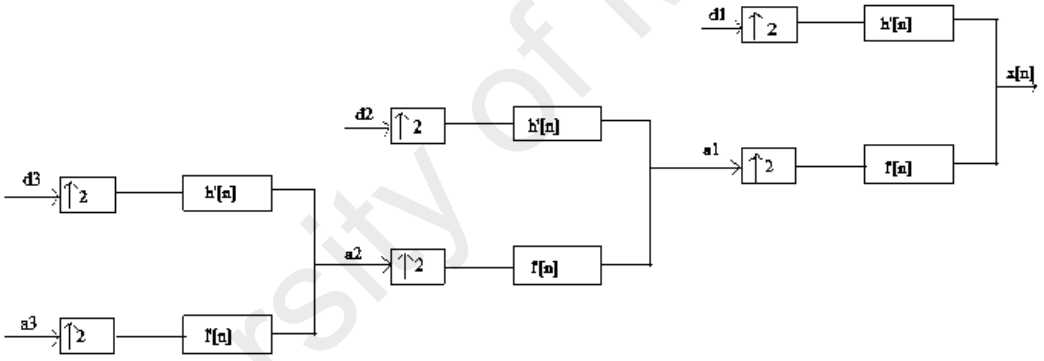


Figure 2.8: DWT reconstruction levels

### 2.5.3 Discrete Fourier transform (DFT)

DFT converts equally-spaced samples of a function of a finite sequence into the same length of sequence for equally-spaced sample of the discrete-time Fourier transform (DTFT). DTFT is complex function of frequency [25]. The space where DTFT is sampled is the reciprocal of the input order duration. An inverse DFT uses DTFT samples as the coefficient of complex sinusoids at appropriate frequencies of DTFT. It has similar sample values as the original input order. The selection of the

optimum mother wavelet and threshold for DWT is important in obtaining good performance of DWT [26].

DFT is the original sequence of a frequency-domain for input data. If the initial sequence expands all non-zero number of a function, the DTFT is periodic and continuous. DFT yields discrete samples of a cycle. If the initial input sequence is a cycle from a periodic function, DFT yields all non-zeroes of a DTFT cycle [27].

DFT is one of the most main discrete transform in Fourier for various applications. In digital signal processing (DSP), the function is a signal or quantity, which changes against time, for example daily temperature readings or radio signal, sound wave pressure, sampled against a time step. In image processing, the samples are the pixels in a column or row of an image.

DFT has been applied to determine partial differential equations and for many operations, for example, multiplying large integers or convolutions. DFT deals with a large amount of data. Hence, it is possible to implement it in computation by numerical methods or a hardware. The implementation applies fast Fourier transform (FFT) method. Hence, the terms DFT and FFT are interchangeable. Before its current usage, FFT has been applied for finite Fourier transform [28].

### 2.5.4 Wavelet packet transform (WPT)

WPT is a good to identify sharp edges of a transition [29]. The signal decomposition using wavelet has a good adaptation to signals with special characteristics [30, 31]. The extension to the adaptive-based characteristics of WPT which a signal is possible, leads to coefficients to a compact representation of signals. When PD is

measured closely to their source, for instance a measurement of PD at a termination, WPT technique is suitable to be used.

Basically, WPT is widely used to denoise PD signals to enhance the detection sensitivity with the assumption that measurements are added with additive white Gaussian noise [32, 33]. Many problems that exist in denoising PD signals for online testing such as selection of threshold value and noise interference from nearby location have been solved [34, 35]. Due to the WPT effectiveness in approximation of PD signals, efforts have been taken to apply WPT in gaining a vector of feature which characterises PD signals from various places. WPT was applied to obtain a frequency-time figure for various PD types, where the decomposition of PD image was obtained using WT for feature extraction [36].

PD signals captured from the experiment were applied into WPT to identify a vector of feature to be applied in the training. Using WPT to determine a vector of feature other than transforming into representation of the signal is better because it can be added with noise reduction within one step and improvement of sensitivity. PD signals are nature of stochastic according to how PDs are obtained. For a PD to happen, 2 conditions must be reached [37]. The electric field is higher than a PD field of inception and one electron is there for a discharge.

WPT transforms can successfully handle random time frequency localization, not like Fourier transform, which time information of a signal is not recovered. WPT coefficients can be applied as features for PD determination and application in sub-band signals to delineate subtle features in a signal. The signal statistical properties of decomposed L2(R) within a wavelet of orthonormal are simplified compared to the statistical properties of the initial signals. Also, the wavelet function

orthogonality can reduce the mathematical analysis. Decorrelated statistical of the wavelet packet coefficients of a band-limited wide-sense stationary with higher resolution is a random process [38].

The level of resolution after the signal is starting to de-correlate is depending on the wavelet moments. Consider a random *x* as a rule for assignment on each output *z* as *x*(*z*). A process of stochastic *x* is a rule to assign to each *z* as a function of *x*(*t*, *z*). Thus, it is a time function family that depends on *z*. *z* is the set of all experimental output and the *t* domain is a real number set *R*. A PD is a complex phenomenon and can be taken as a stochastic phenomenon, which is unable to be described by a finite parameter numbers. A stochastic phenomenon can be defined in term of the order *k* cumulant by

$$\text{cum}(x(t1), x(t2), x(t3), x(t4), x(tk)) = Ck(t1, \dots, tk) \tag{2.10}$$

Therefore, the first four cumulants of this process are

$$\begin{aligned} C_1(t) &= E[x(t)] \\ C_2(t_1, t_2) &= E[(x(t_1)(x(t_2)] \\ C_3(t_1, t_2, t_3) &= E[x(t_1)x(t_2)x(t_3)] \\ C_4(t_1, t_2, t_3, t_4) &= E[x(t_1)x(t_2)x(t_3)x(t_4)] \end{aligned} \tag{2.11}$$

The stochastic process cumulants are multi-dimensional vectors, which are difficult to be visualised and processed. It is commonly used in processing of signal to yield a 1 dimensional slice through freezing some of its indexes *k*. A lot of types of 1 dimensional slice are available, which include horizontal, vertical, offset and radial, diagonal.

The wavelet coefficient at every level was considered as a stochastic process. Hence, the cumulants depending on the level for the coefficients of wavelet were gained

through WPT on each data. Every stochastic process was approximated by the standard deviation, skewness, mean and kurtosis at every decomposition node. To decrease the feature vector dimensionality belonging to decomposition, similar scale was added and was applied for every PD type as a fingerprint and used as the input for the classifiers. The kurtosis, standard deviation, mean and skewness are calculated using

$$\eta = \frac{1}{N}\sum_{n=1}^{N}(x[n]) \tag{2.12}$$

$$\sigma = \left(\frac{1}{N}\sum_{n=1}^{N}(x[n]-\eta)^2\right)^{1/2} \tag{2.13}$$

$$\gamma = \frac{1}{N\sigma^3}\sum_{n=1}^{N}(x[n]-\eta)^3 \tag{2.14}$$

$$\kappa = \frac{1}{N\sigma^4}\sum_{n=1}^{N}(x(n)-\eta)^4 \tag{2.15}$$

where $x[n]$ is the wavelet coefficient at position $n$ and $N$ is the wavelet coefficients number used at every scale.

An assumption of one AC cycle has one PD only with a one type and of a single source is based on the limitation of the method the signals were captured and the classification algorithm and vector of the feature was validated. The classification algorithm and vector of the feature were applied to deal with PD sources of many sources. The classification under many PD sources in one AC cycle was investigated in [39].

# CHAPTER 3: METHODOLOGY OF THE WORK

This chapter describes the methodology that has been used for this work. PD measurement method, sample preparation for PD measurement and the proposed PD type classification techniques are described in details. This work focuses on obtaining PD patterns from five types of commonly encountered defect in actual XLPE cable joints and performing classification to identify the defect. Feature extractions were performed to obtain useful input features, which serve as identification marker for the cable joint defect. The extracted features of the input were implemented as the input data for SVM classifier.

Different noise levels with increasing pulse count and magnitude were added to the PD signals to observe which input feature and classifier has the higher noise tolerance. The classifiers were trained using noise-free PD signals but tested with noisy PD signals. Noise levels of variable pulse count and noise level with variable amplitude were tested. The noise source was obtained from ground interference during raining which is not a randomly generated noise.

## 3.1 Flowchart of Work

The work was started with the measurement of PD signals in a laboratory as shown in Figure 3.1. There are five XLPE cable joints prepared in the lab, as shown in Table 3.1. Each of them was measured using the applied voltage of 6kV, 7kV and 9kV for comparison on which defects have more PDs and to recognize them through different applied voltage. Next, PD patterns were recorded for each of the sample.

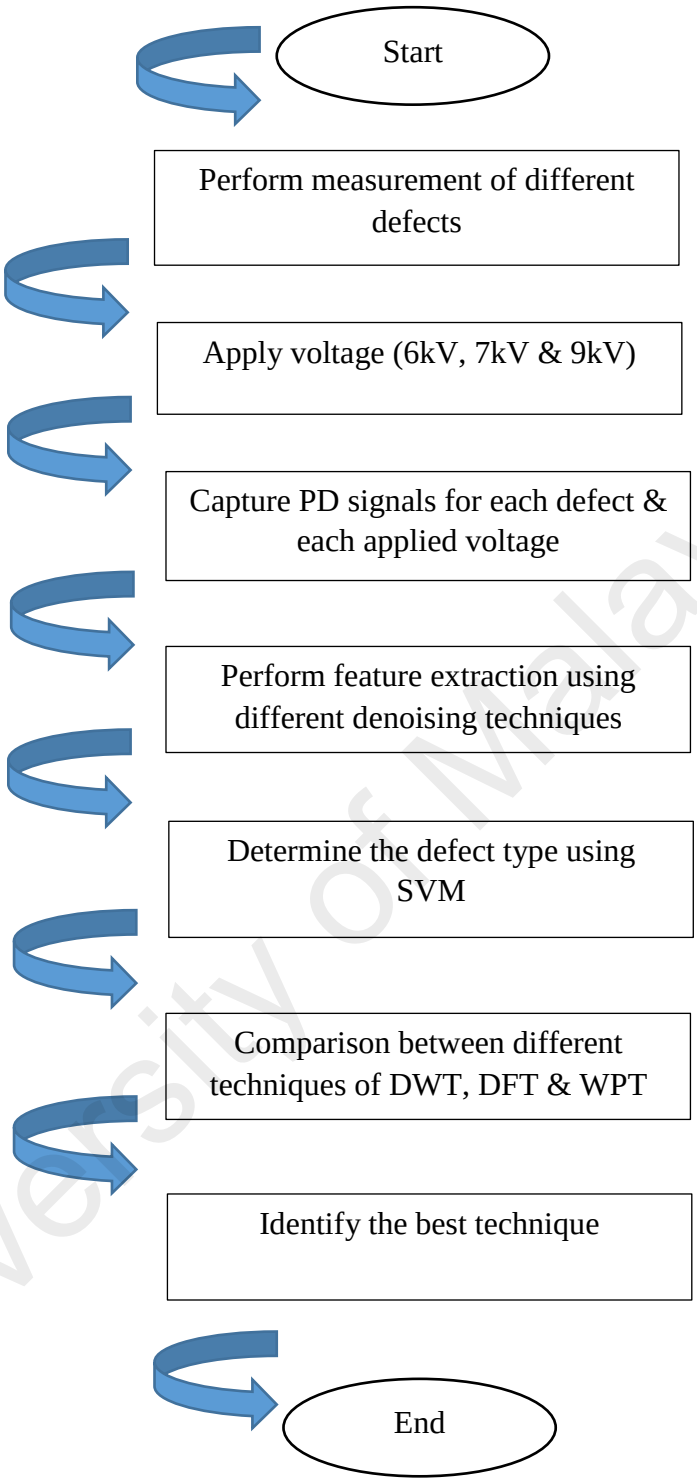


Figure 3.1: Flowchart of laboratory test work

## 3.2 Samples Prepared

Five XLPE, 11 kV cable joint with various defects artificial created were prepared as shown in Table 3.1. Defect of semiconductor layer air gap was introduced with

insulation tape to wrap air layer around the semiconductor edge. Defect of metal particle on XLPE was introduced by spreading metal particles on the XLPE layer. Defect of insulation incision was introduced by using a shallow cut at the XLPE layer with a sharp knife. Defect of semiconductor layer tip was introduced by using rough edges at the semiconductor tip. Defect of axial direction shift was introduced by including the cable at an angle of out of centre. All defects were made at the XLPE cable before the joints were installed. The pictures of the defects are shown in Figure 3.2.

Table 3.1: Cable joint defects used for the experiment

| Cable Joint | Defect type |
|---|---|
| C1 | Defect of incision in insulation |
| C2 | Defect of shift in axial direction |
| C3 | Defect of tip at semiconductor layer |
| C4 | Defect of XLPE metal particle |
| C5 | Insulation cable with no defect |

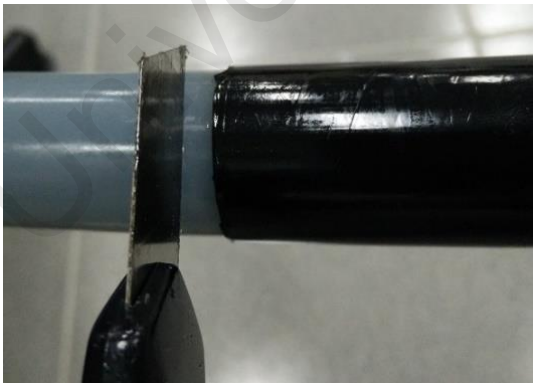

(a)

(b)

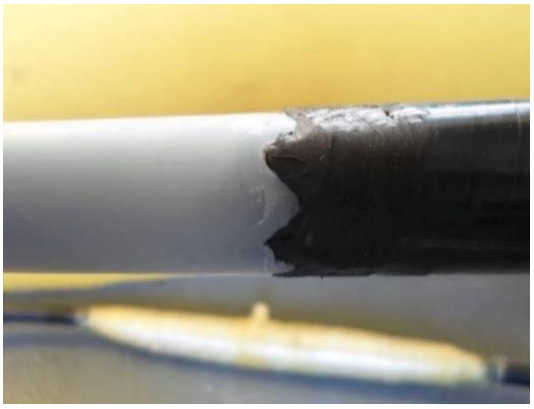

(c)

(d)

(e)

Figure 3.2: Defects created; (a) Defect of incision on insulation, (b) Defect of shift on axial direction, (c) Defect of tip on semiconductor layer, (d) Defect of XLPE metal particle and (e) Defect of air gap in semiconductor layer

### 3.3 PD Measurement

Figure 3.3 shows a schematic diagram of a typical PD measurement set up and Figure 3.4 shows the actual measurement setup in HV laboratory. It consists of HV source served by step up transformer, measuring capacitor, cable joint sample, a coupling capacitor and a coupling device and a PD detection unit connected to a PC by a USB controller. The mobility of the charge from coupling capacitor produces a current, which is measured by the PD detector. The coupling device converts the detected current to a voltage. PD measurements taken from the different defects were performed at 6kV, 7kV and 9kV to identify the PD pattern at the PC.

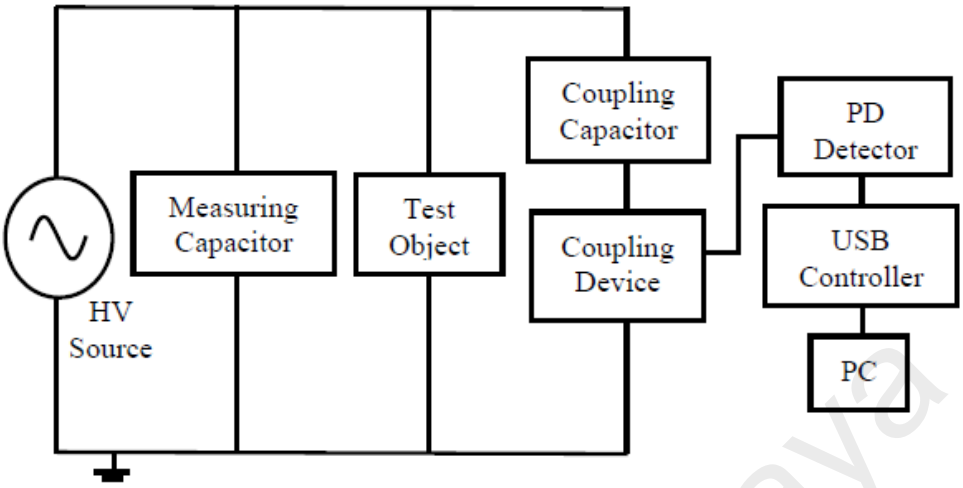


Figure 3.3:Setup of PD measurement under AC voltage

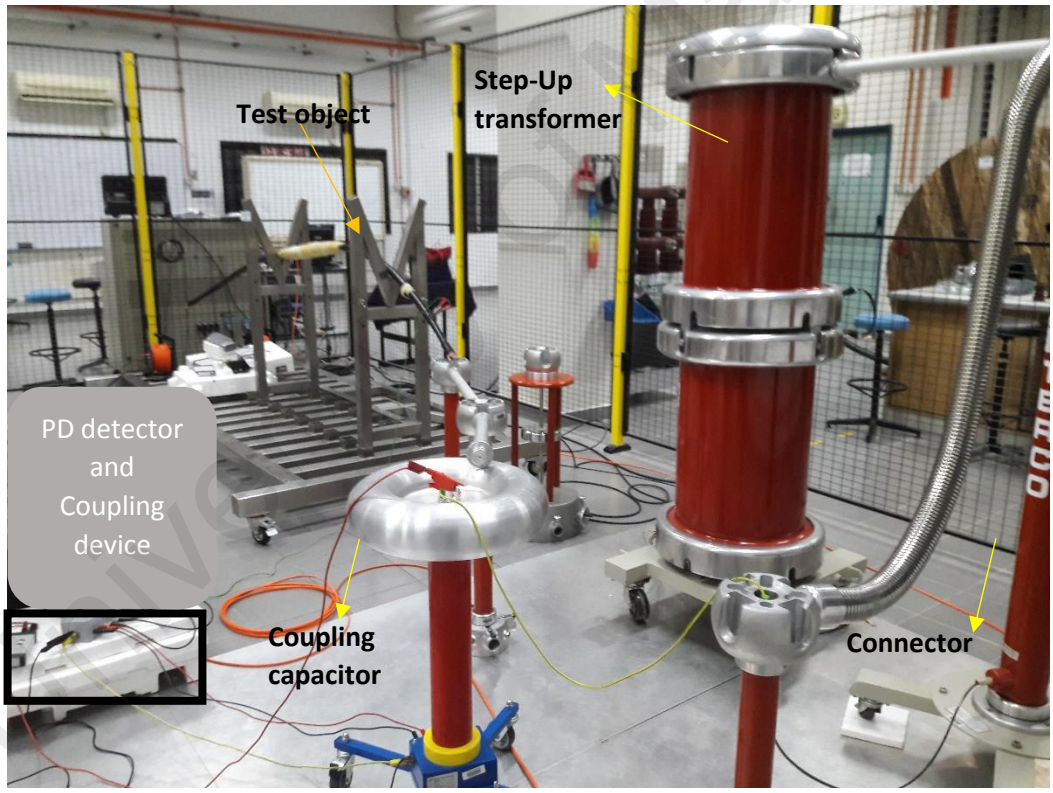


Figure 3.4: PD measurement setup in HV laboratory

The measurement was started with insulation incision defect. Each defect was measured one by one using different source voltage such as 6kV, 7kV and 9kV. Thus, each of the defect was tested three times to obtain the PD pattern. The pattern

was stored in a PC and the PD signals were transferred from the testing devices to PD detector.

### 3.4 Methods of PD classification

In this work, PD classifier used to classify the PD signals is SVM. As the signal to noise (SNR) is higher it means lower noise. Denoising tehcniques used were DWT, DFT and WPT and were compared to between each other. The SVM method used is as shown in Figure 3.5.

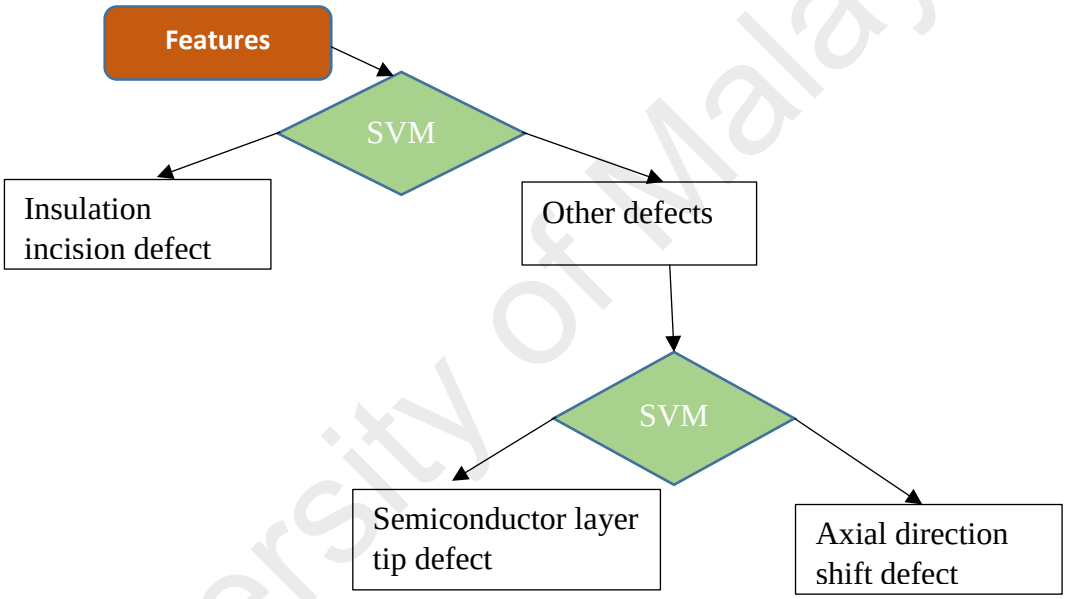


Figure 3.5: Feature concept of SVM

### 3.5 Denoising techniques of PD signals

Three techniques used to measure the PD signals are shown in Figure 3.6. Each of them consists of clean, noisy and denoised PD signals. The result was obtained by measurement of the PD signals using different techniques. The accuracies of the three techniques were determined.

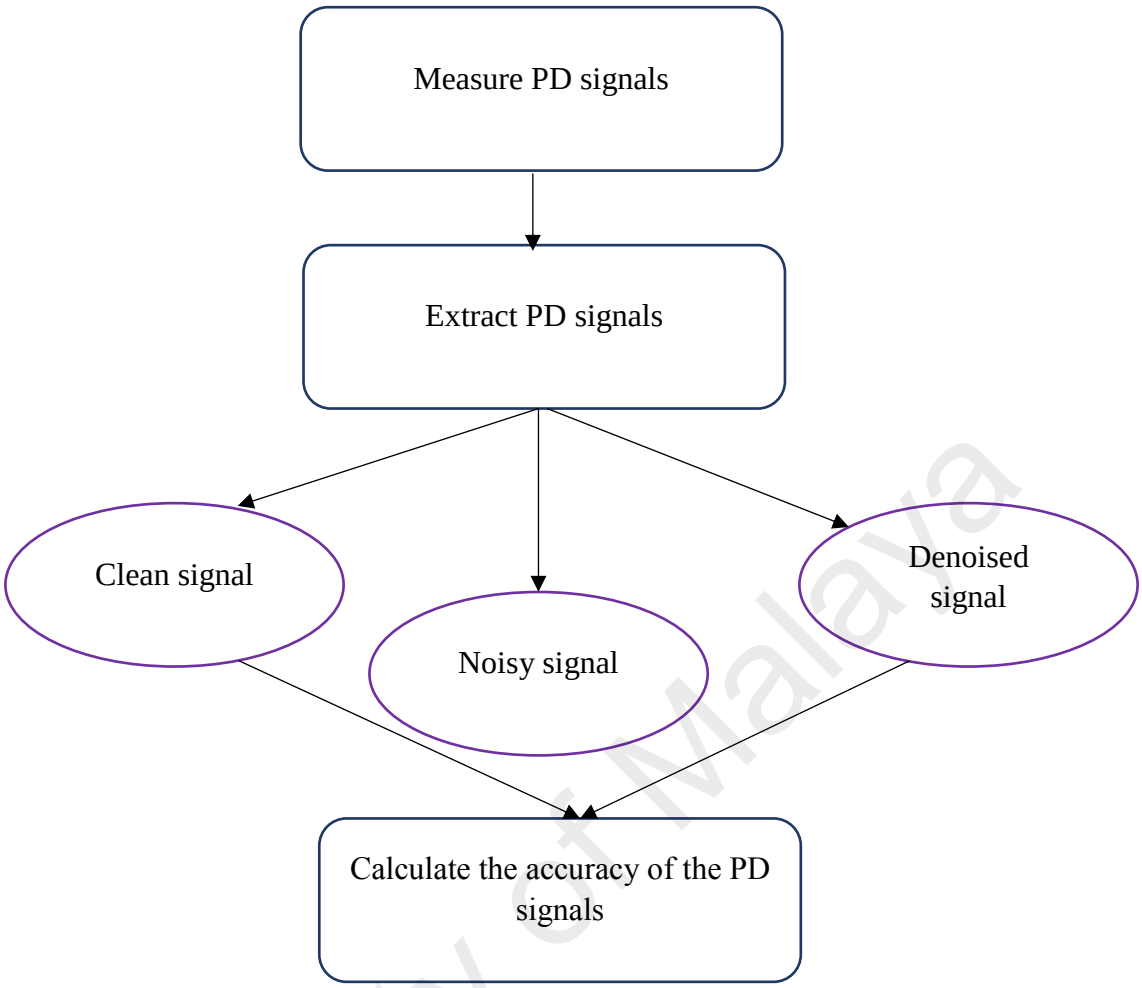


Figure 3.6: Denoising techniques flowchart

# CHAPTER 4: RESULTS AND ANALYSIS

## 4.1 OMICRON software

PD signals from each defect were obtained using OMICRON software. The MPD600 detector allows stream signals of PC to be displayed without using an oscilloscope. It is interfaced to display the signals in different ways, such as phase resolved PD patterns.

Then, the obtained patterns were exported into MATLAB and Excel for further data analysis. By having the OMICRON software, the signals can be displayed and recorded. Figure 4.1 shows a view of the MPD600 software, which was used in the experiment according to the IEC60270 standard recommendation. Every defect was examined and tested using the same configuration of the PD threshold and the time for histogram acquisition was set to one minute.

## 4.2 Measured PD signals

PD signals were recorded for the five different defects of XLPE cable. Figures 4.2 to 4.5 show the results of PD patterns at 6kV, 7kV and 9kV for each of the defects. The figure indicates the PD signals from insulation incision, axial direction shifts, XLPE metal particle, air gap in nsemiconductor layer and semiconductor layer tip defects.

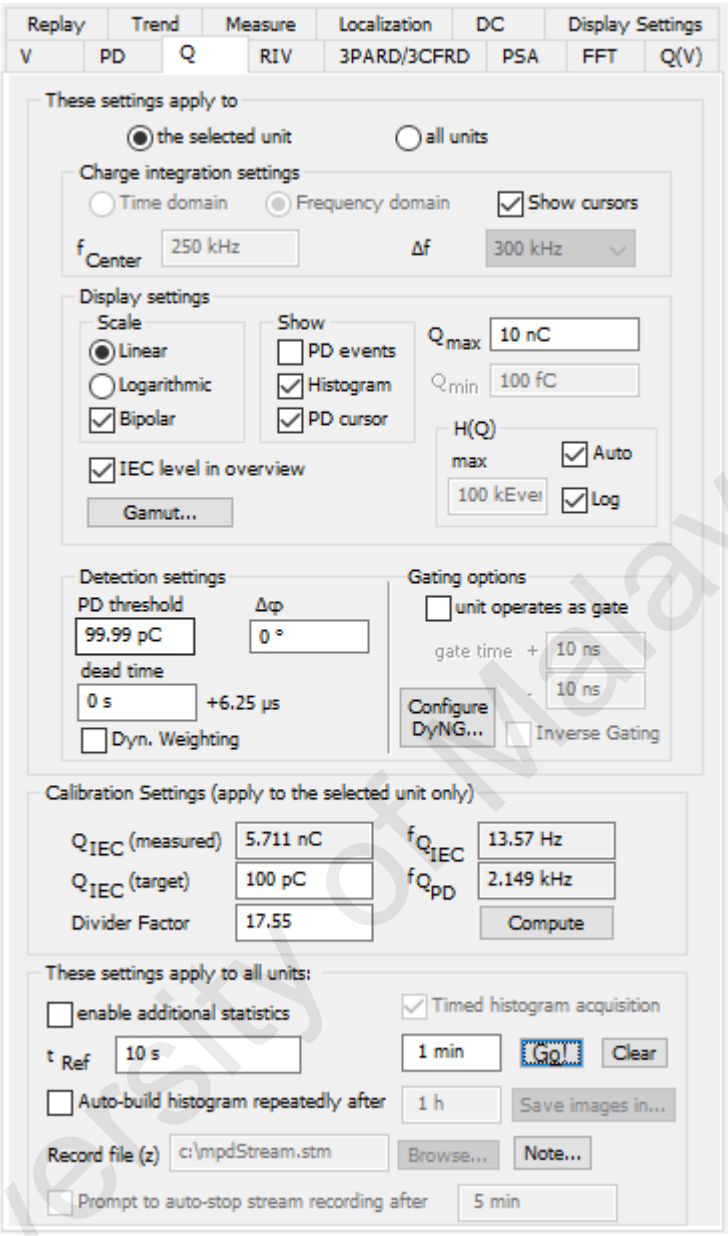


Figure 4.1: Setup of MDP600 software

## 4.3 Results obtained using OMICRON MPD600 software

Using the MPD600 software, the PD patterns were recorded and captured for each defect to see the differences in the PD patterns. Figure 4.2 shows that as the voltage increased to 9kV, the number of PD increases to 94% from 92% and 93% for defect C1 (insulation incision defect). The pattern of the PD signals can be seen clearly as increasing as the voltage is increased.

For Figure 4.3, the increasing number of PD signals was detected at the increasing voltage to 9kV for defect C2 (axial direction shift defect). Referring to the PD pattern in this figure, the PD signals showed at 93% but it is obviously shown the increasing of PD pattern at the increasing voltage from 6kV to 9kV. Larger difference in the percentage of the PD number can be seen if the voltage is increased higher.

From Figures 4.4 and 4.5, the percentage of PD signals is 95% and 86% respectively. Table 4.1 shows the percentage at 9kV of the applied voltage for the four defects, which are C1 (defect of incision on insulation), C2 (defect of shift of axial direction), C3 (defect of tip in semiconductor layer) and C4 (defect of XLPE metal particle).

Table 4.1: PD signals percentage for the four defects at 9kV

| Types of defect | Percentage of PD signals (%) |
|---|---|
| C1 | 94 |
| C2 | 93 |
| C3 | 95 |
| C4 | 86 |

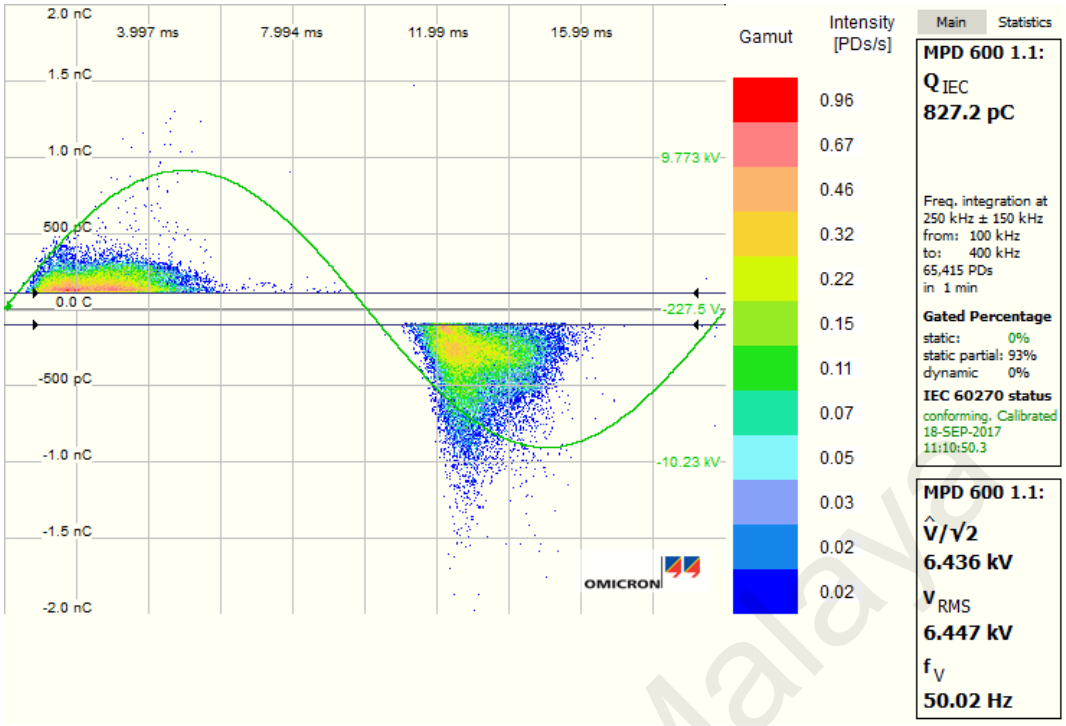


(a)

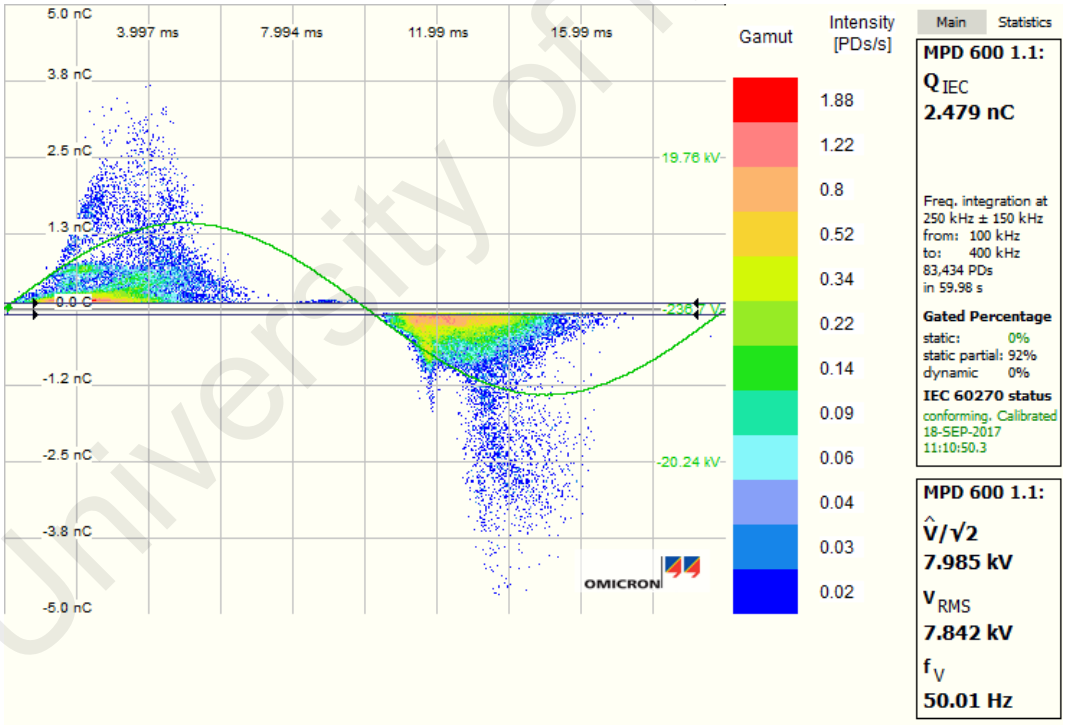


(b)

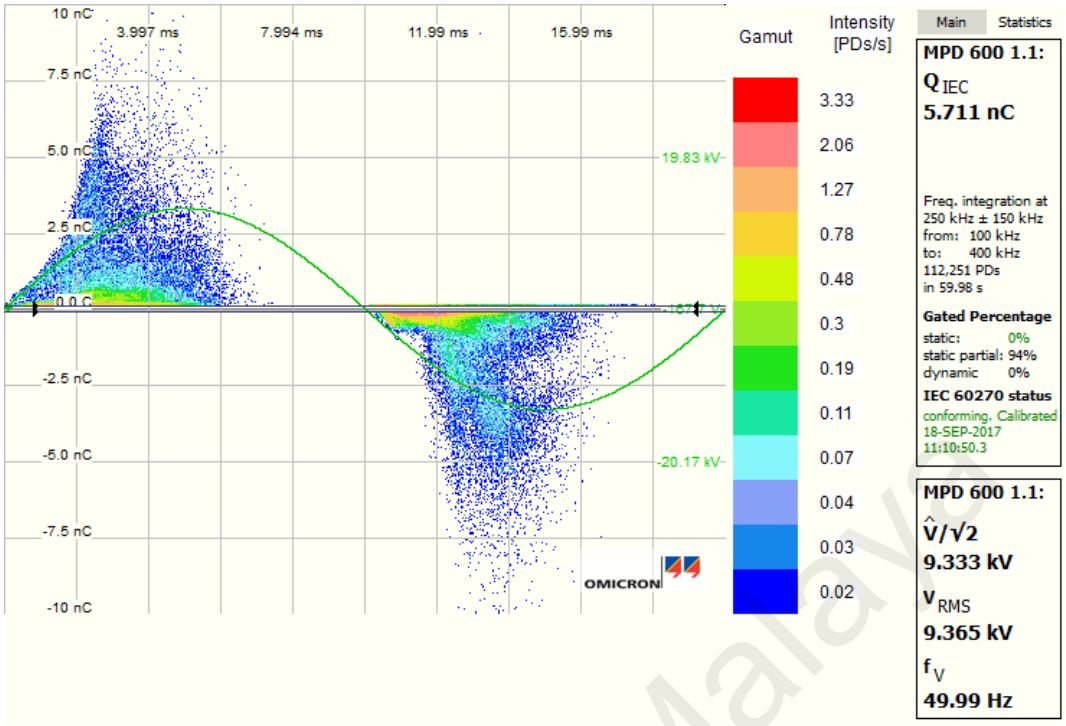


(c)

Figure 4.2: PD pattern on defect C1 (a) 6kV, (b) 7kV and (c) 9kV

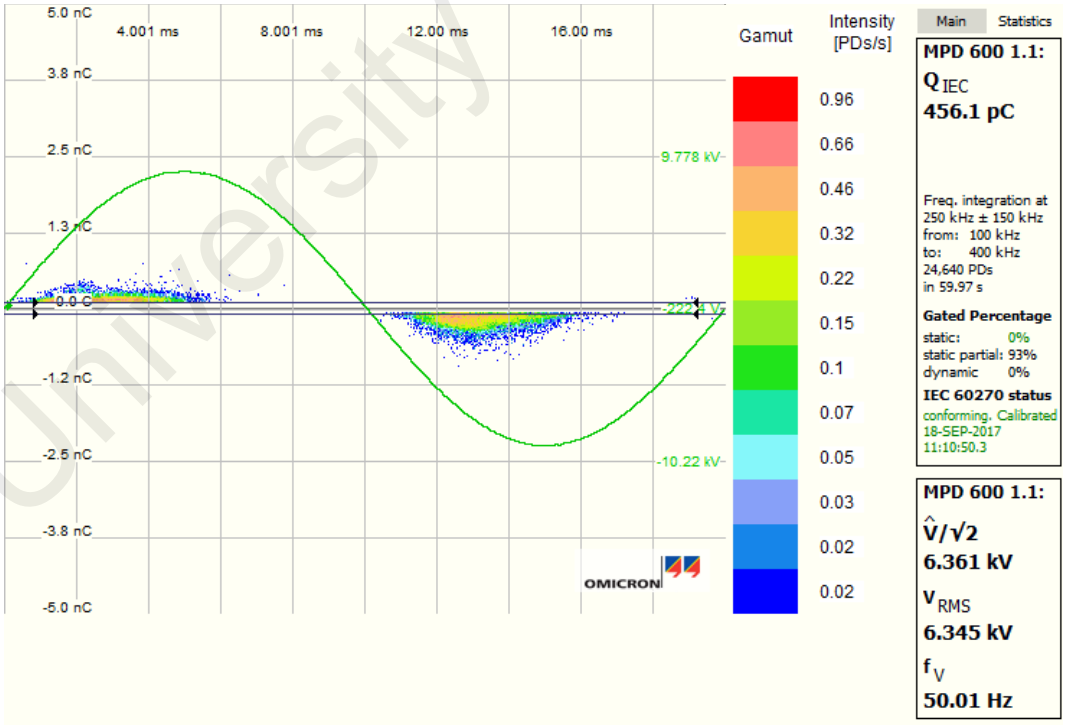


(a)

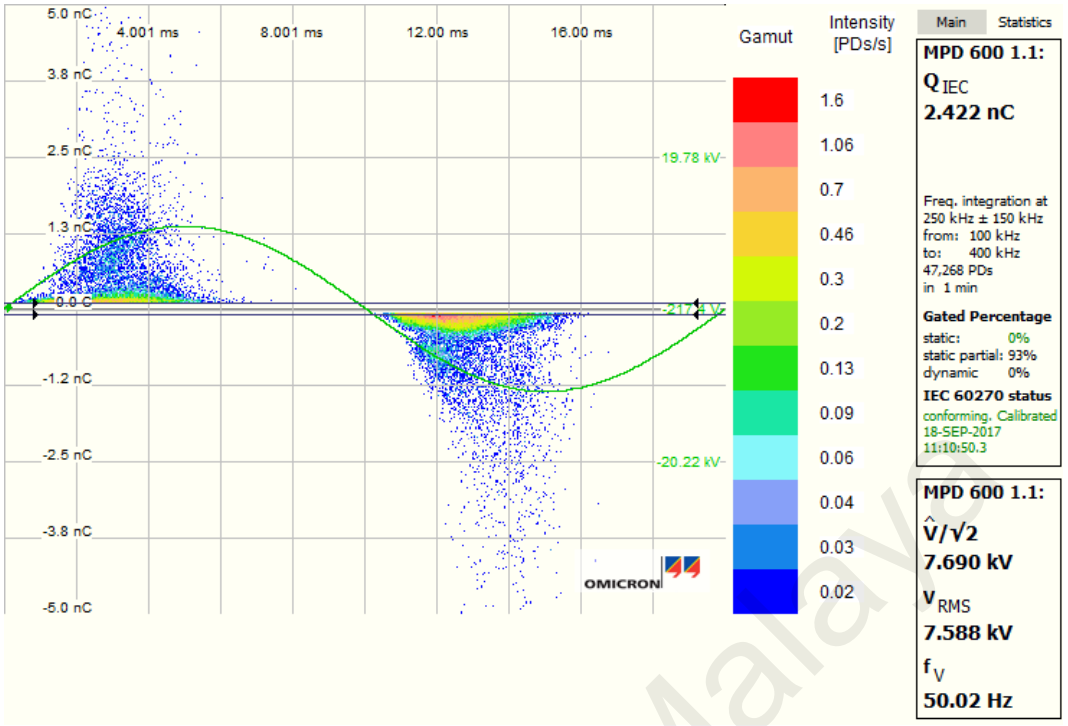


(b)

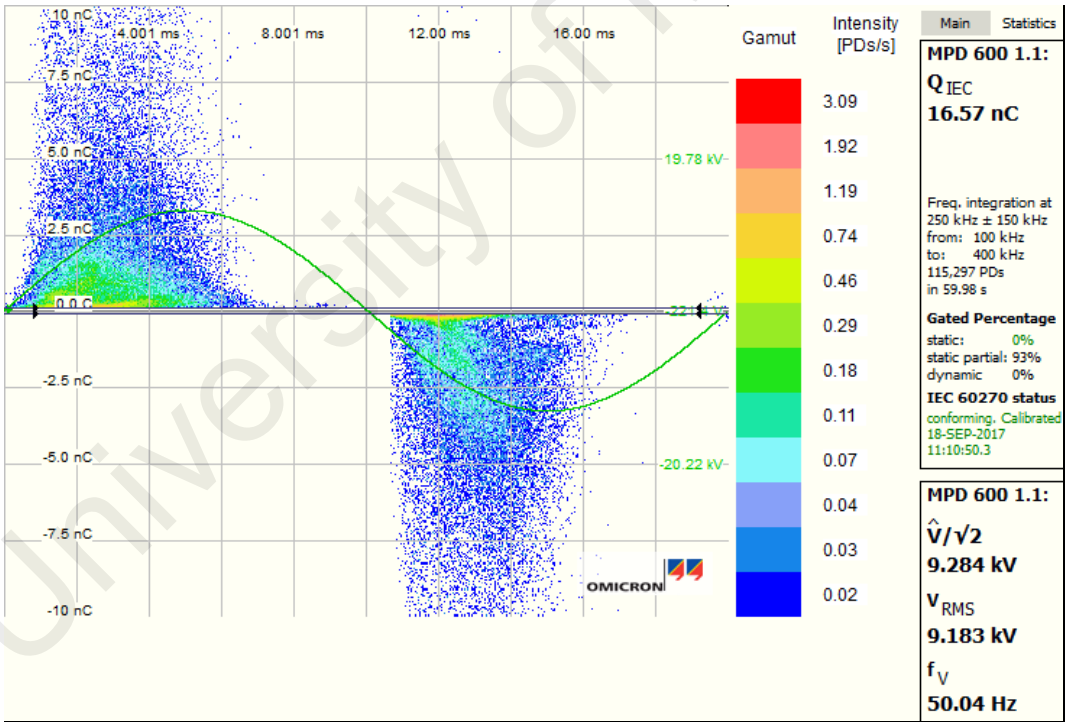


(c)

Figure 4.3: PD pattern on defect C2 at voltage in kV: (a) 6, (b) 7 and (c) 9

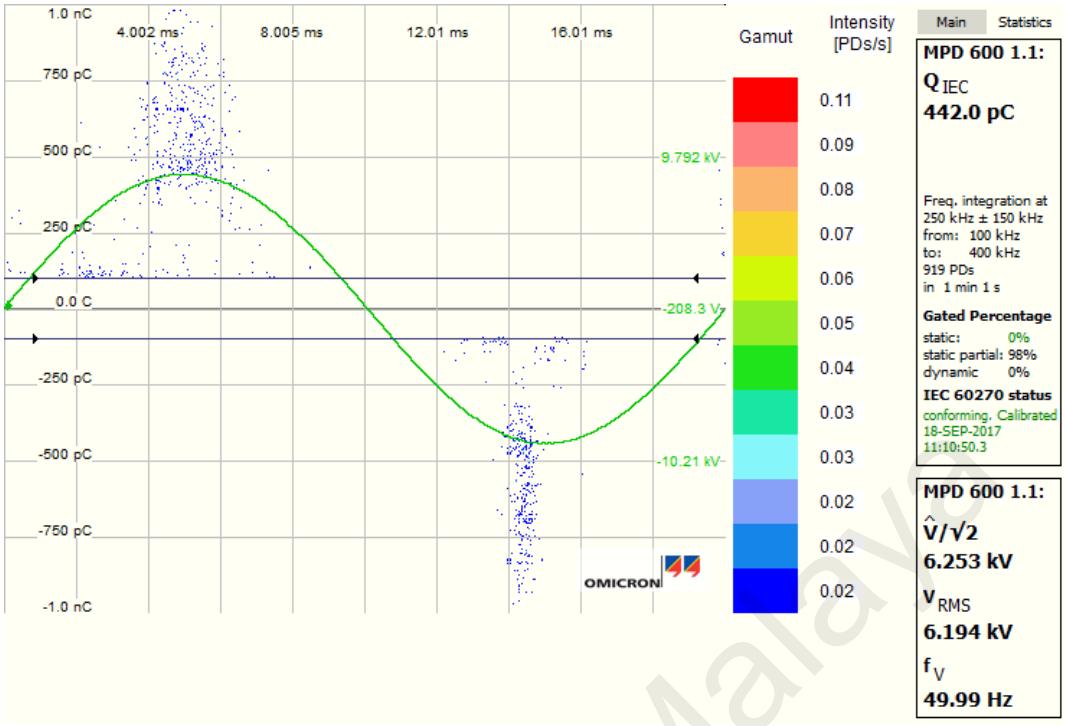


(a)

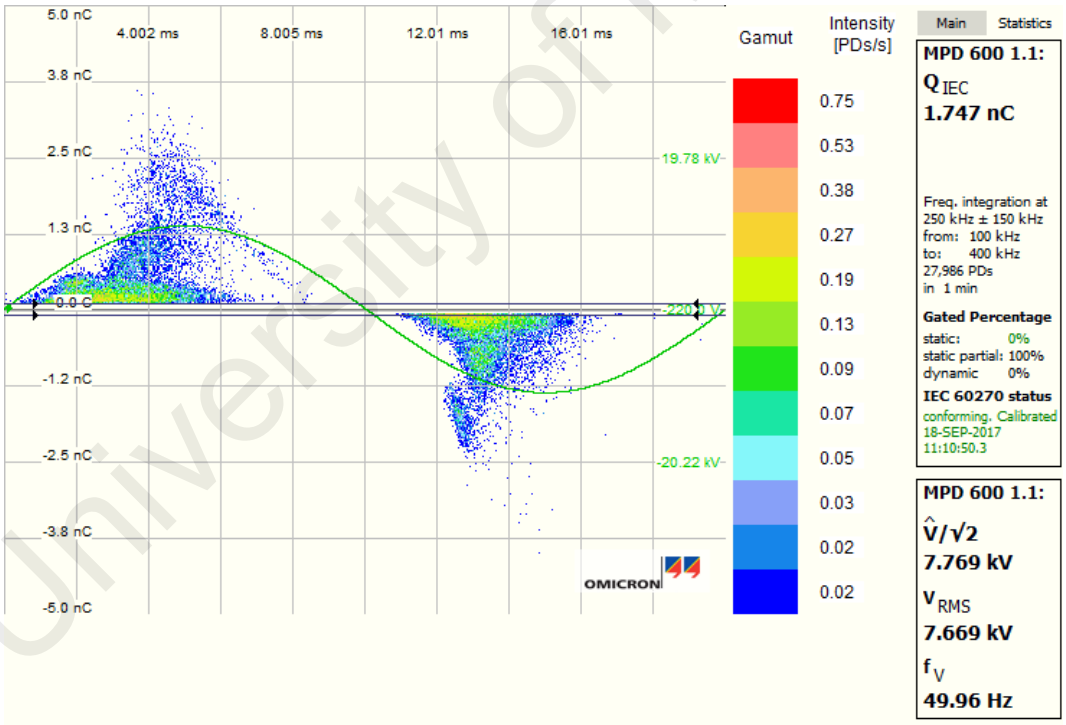


(b)

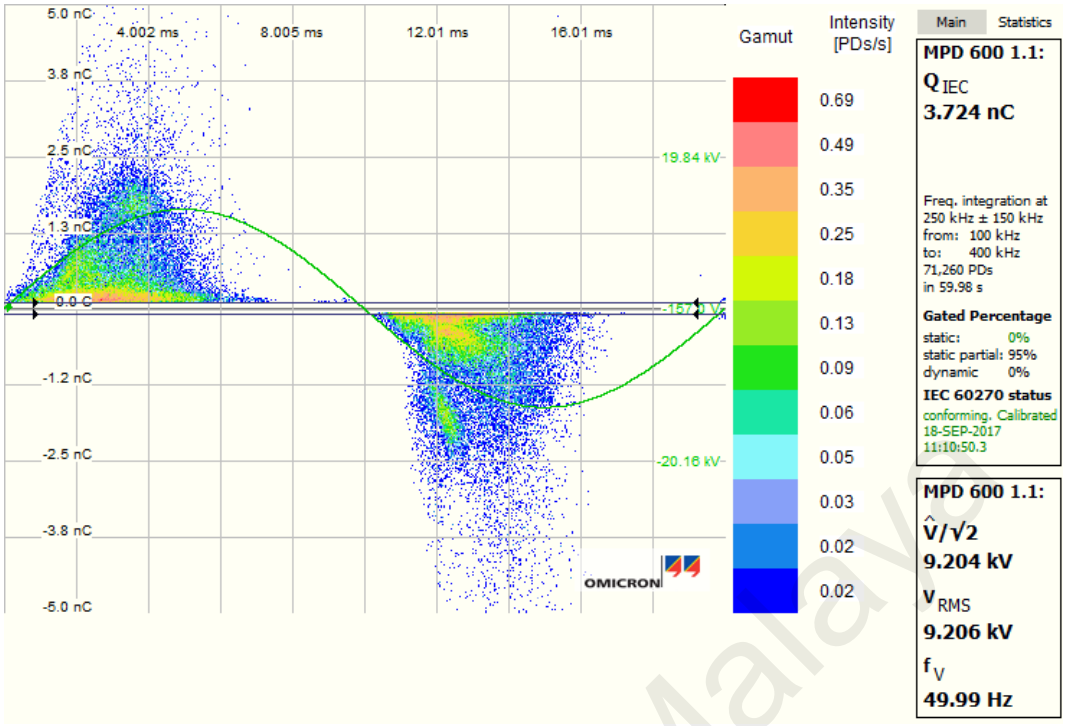


(c)

Figure 4.4: PD pattern on defect C3 at voltage in kV: (a) 6, (b) 7 and (c) 9

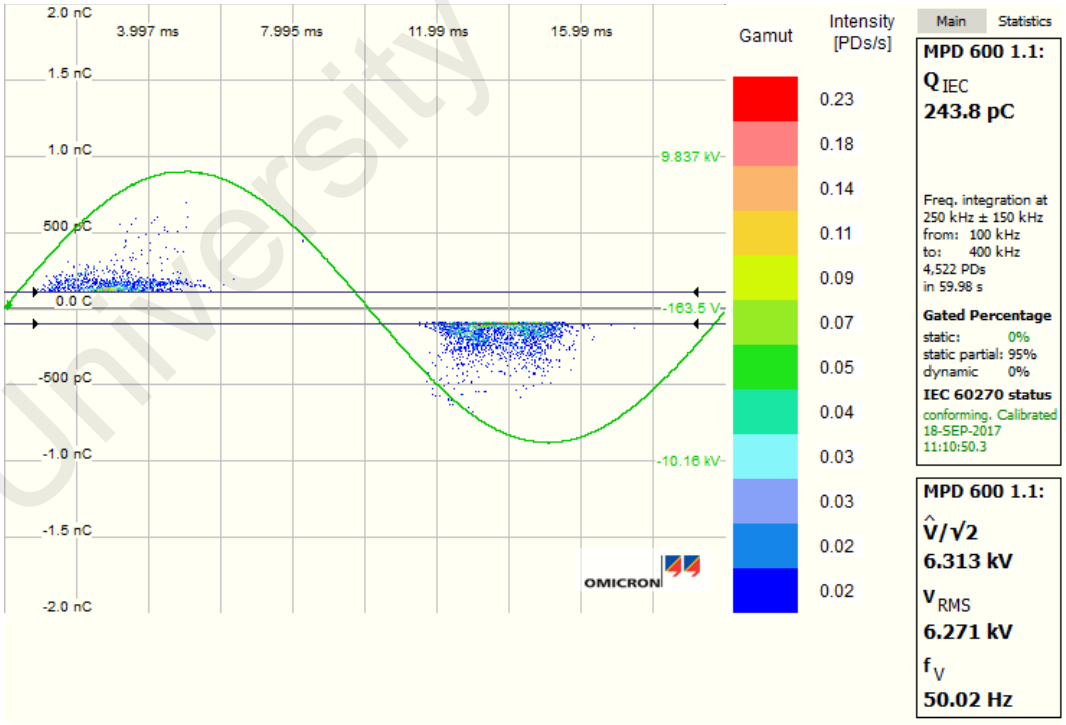


(a)

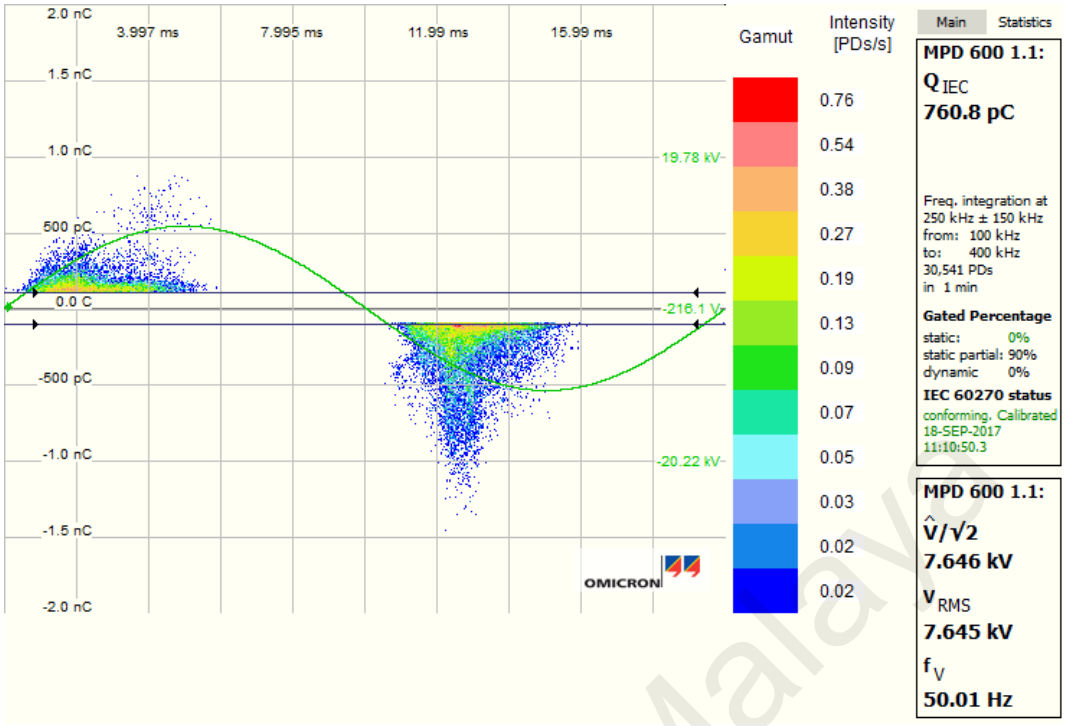


(b)

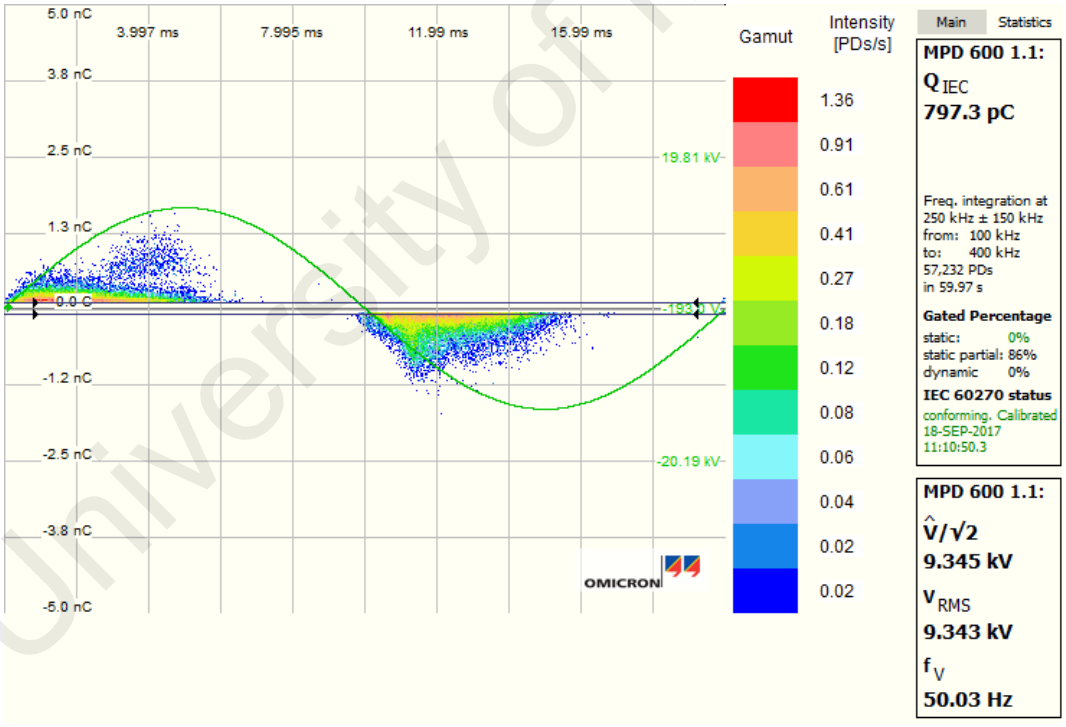


(c)

Figure 4.5: PD pattern on defect C4 at voltage in kV: (a) 6, (b) 7 and (c) 9

## 4.4 Measured PD signals

There are three denoising techniques of PD signals been used in this study, which are DFT, WPT and DWT. Each of the technique was applied to denoise PD signals. The percentage of accuracies was obtained and compared.

### 4.4.1 DFT technique

Figure 4.6 shows a clean PD signal, PD signal after adding noise and denoised signal using DFT for defect C1 (insulation incision defect). Figure 4.7 shows a clean PD signal, PD signal with noise and denoised signal using DFT for defect C2 (axial direction shift defect). Figure 4.8 shows a clean PD signal, PD signal after adding noise and denoised signal using DFT for defect C3 (semiconductor layer tip defect).

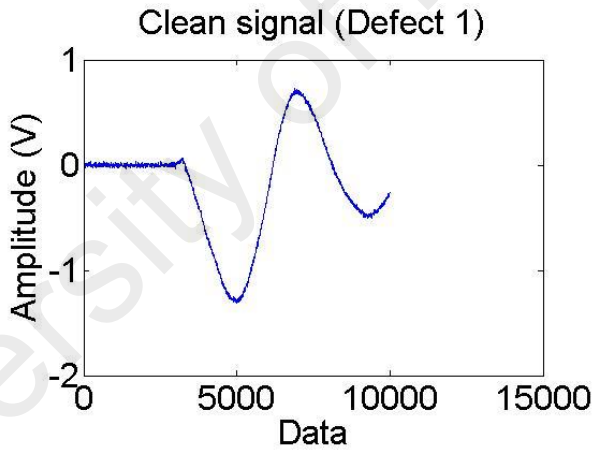


(a)

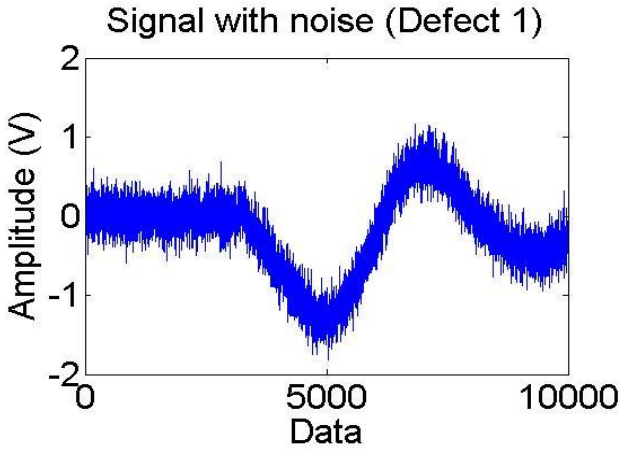


(b)

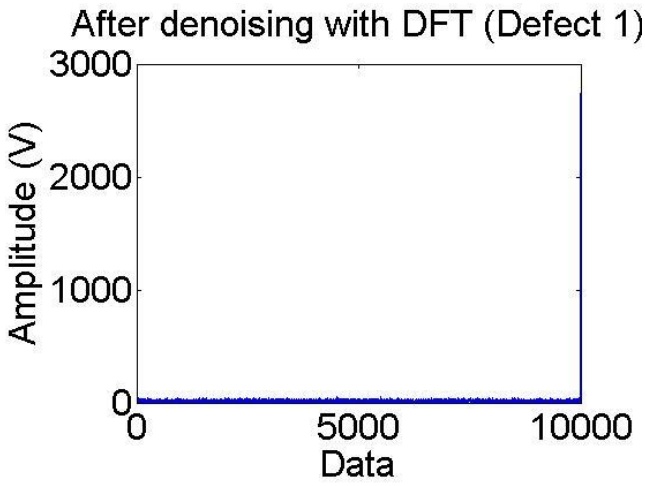


(c)

Figure 4.6: (a) Clean PD signal, (b) PD signal after adding noise and (c) denoised signal using DFT for defect C1 (insulation incision defect).

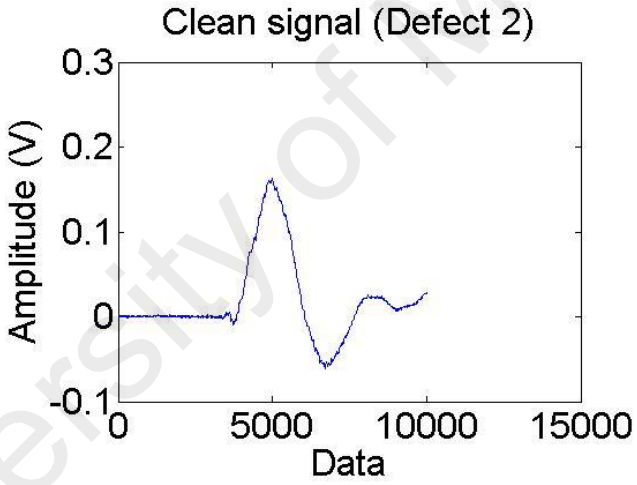


(a)

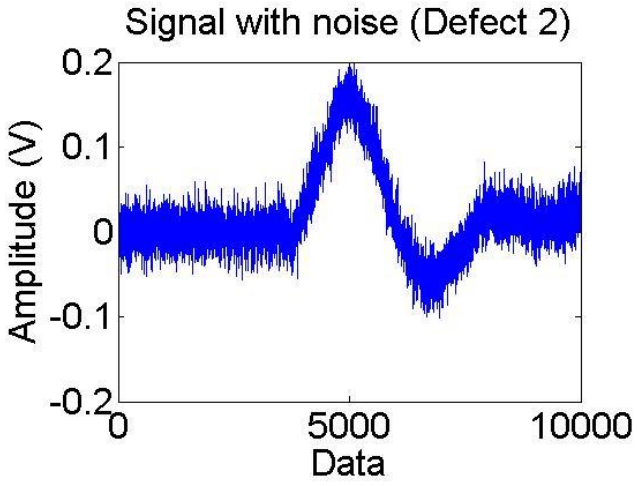


(b)

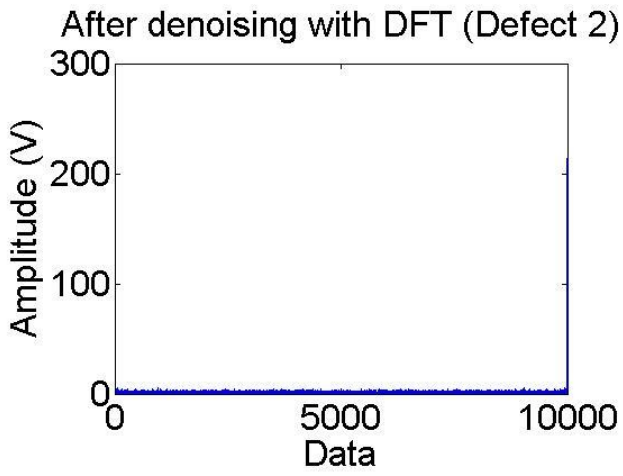


(c)

Figure 4.7: (a) Clean PD signal, (b) PD signal after adding noise and (c) denoised signal using DFT for defect C2 (axial direction shift defect).

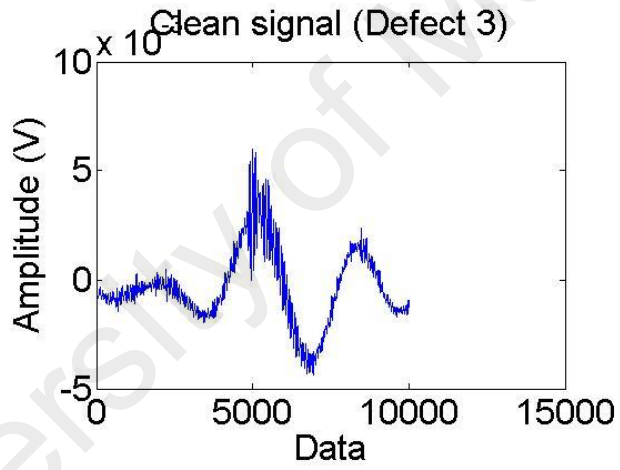


(a)

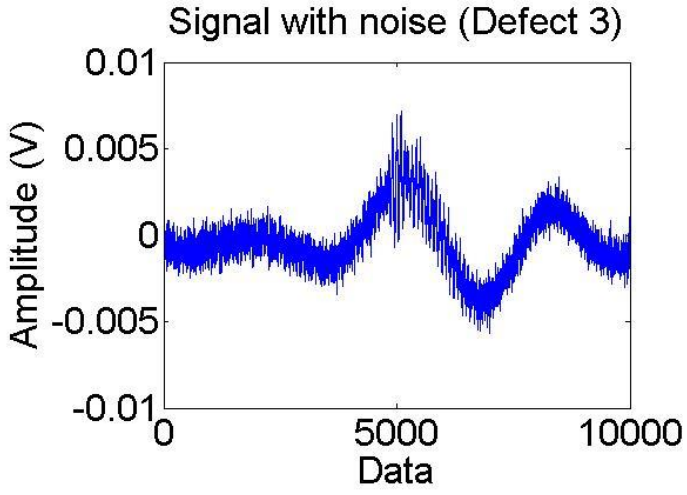


(b)

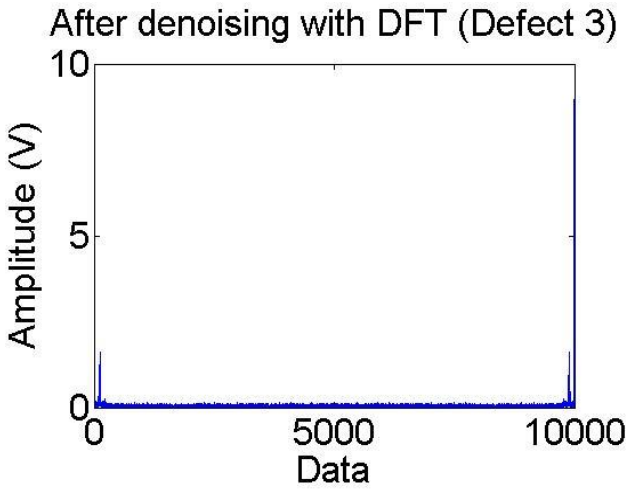


(c)

Figure 4.8: (a) Clean PD signal, (b) PD signal after adding noise and (c) denoised signal using DFT for defect C3 (semiconductor layer tip defect).

### 4.4.2 DWT Technique

Figure 4.9 shows a clean PD signal, PD signal after adding noise and denoised signal using DWT for defect C1 (insulation incision defect). Figure 4.10 shows a clean PD signal, PD signal after adding noise and denoised signal using DWT for defect C2 (axial direction shift defect). Figure 4.11 shows a clean PD signal, PD signal after adding noise and denoised signal using DWT for defect C3 (semiconductor layer tip defect).

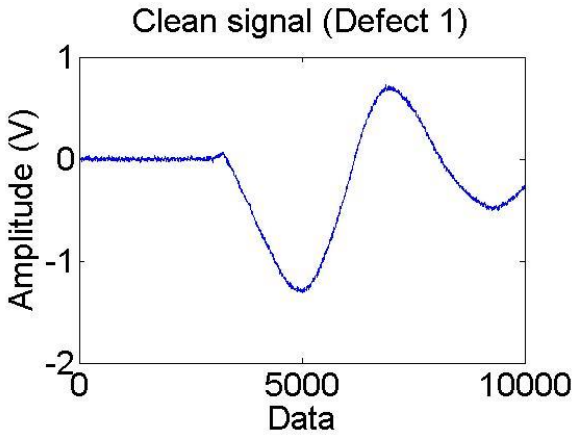


(a)

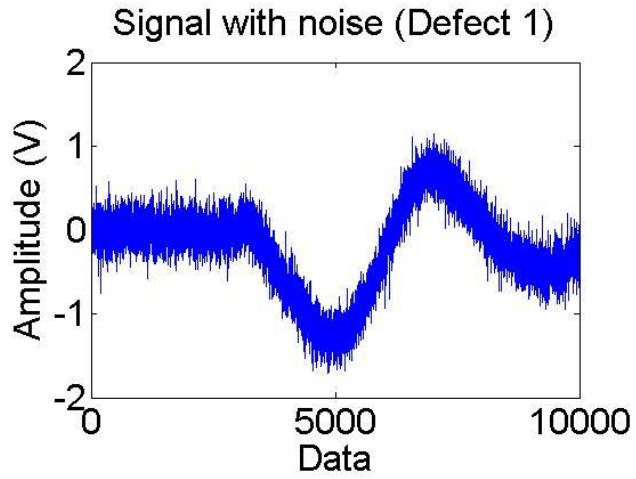


(b)

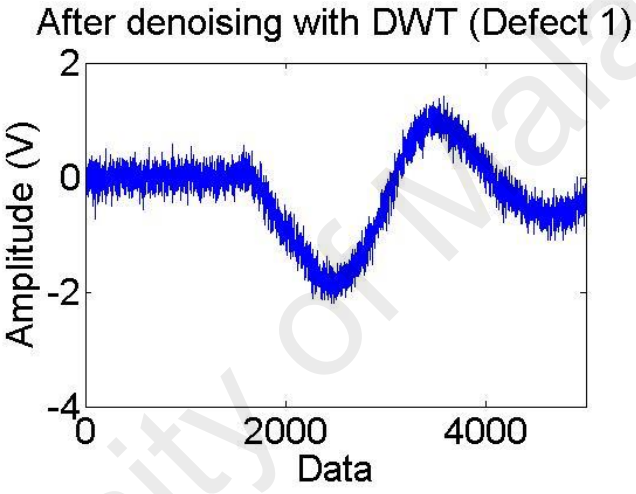


(c)

Figure 4.9: (a) Clean PD signal, (b) PD signal after adding noise and (c) denoised signal using DWT for defect C1 (insulation incision defect).

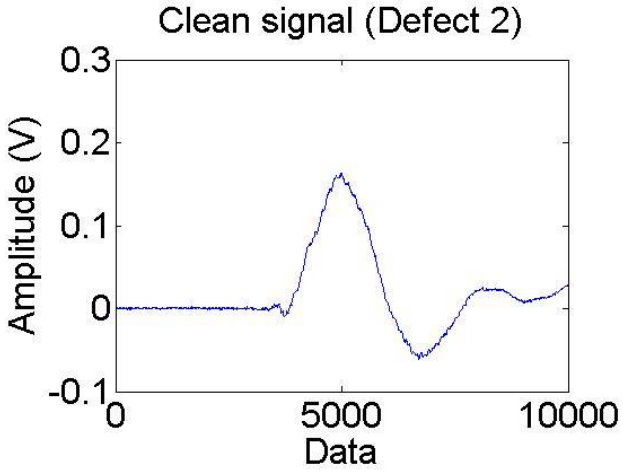


(a)

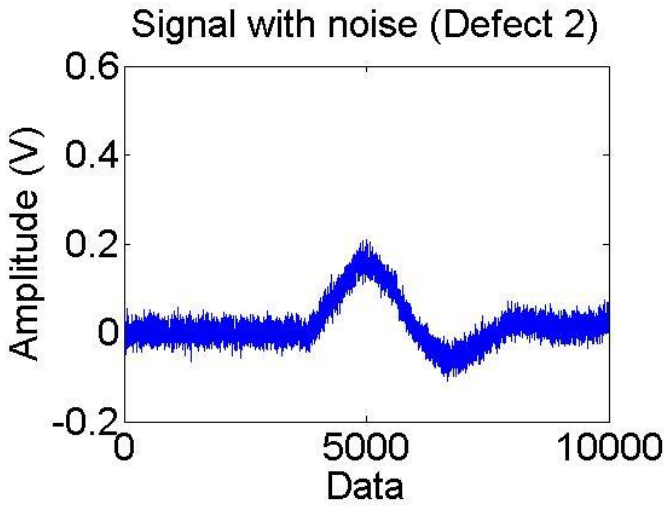


(b)

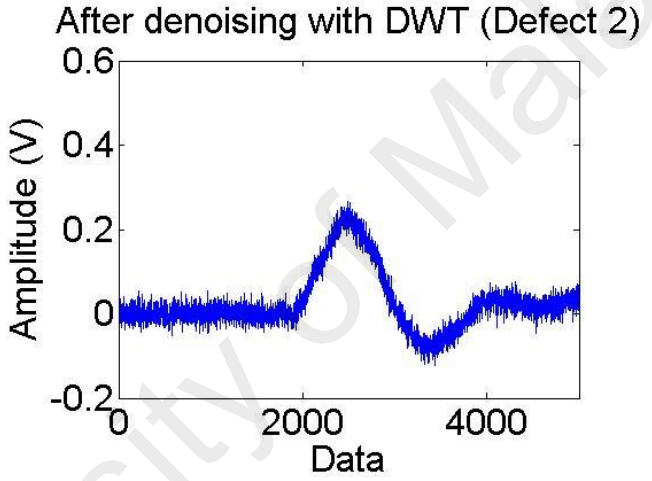


(c)

Figure 4.10: (a) Clean PD signal, (b) PD signal after adding noise and (c) denoised signal using DWT for defect C2 (axial direction shift defect).

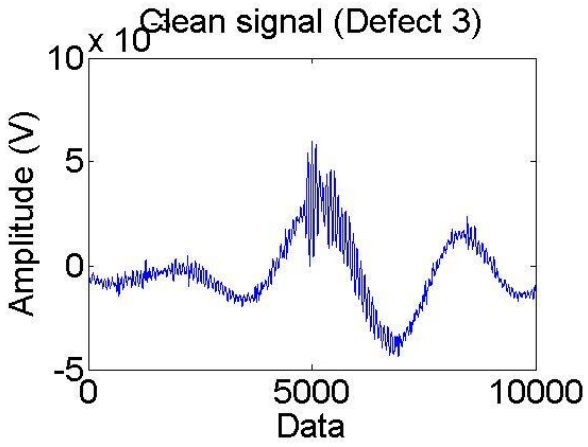


(a)

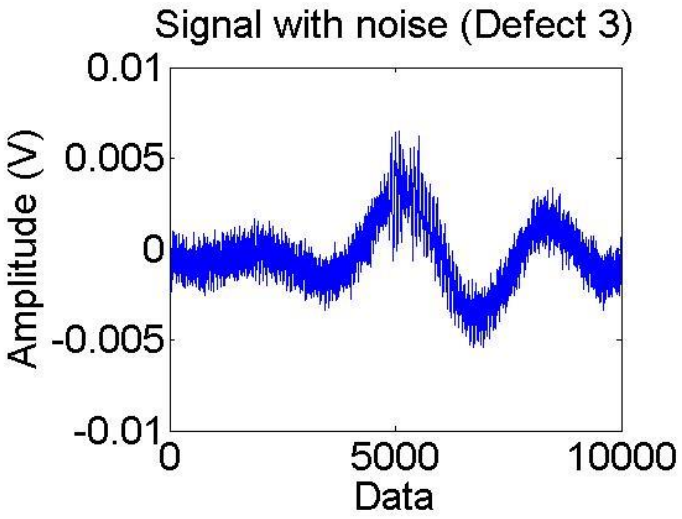


(b)

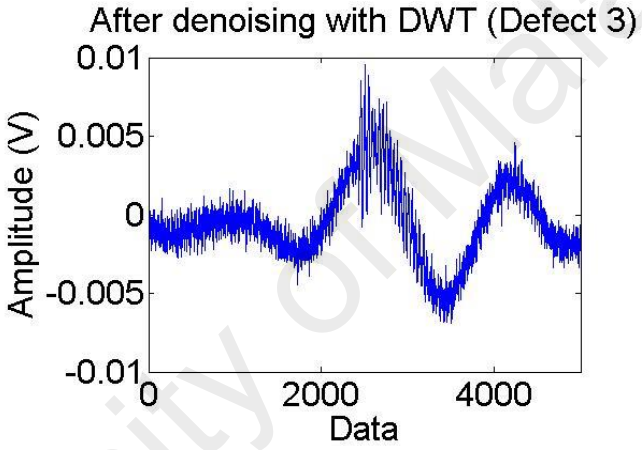


(c)

Figure 4.11: (a) Clean PD signal, (b) PD signal after adding noise and (c) denoised signal using DWT for defect C3 (semiconductor layer tip defect).

### 4.4.3 WPT technique

Figure 4.12 shows a clean PD signal, PD signal after adding noise and denoised signal using WPT for defect C1 (insulation incision defect). Figure 4.13 shows a clean PD signal, PD signal after adding noise and denoised signal using WPT for defect C2 (axial direction shift defect). Figure 4.14 shows a clean PD signal, PD signal after adding noise and denoised signal using WPT for defect C3 (semiconductor layer tip defect).

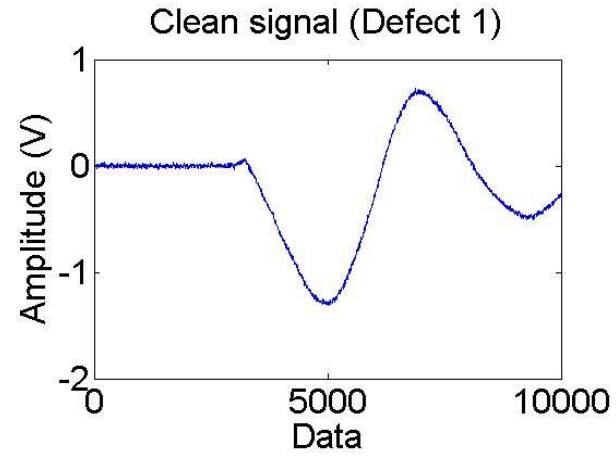


(a)

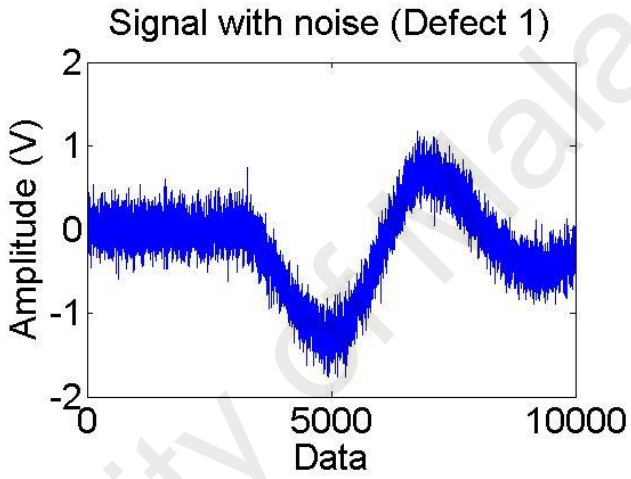


(b)

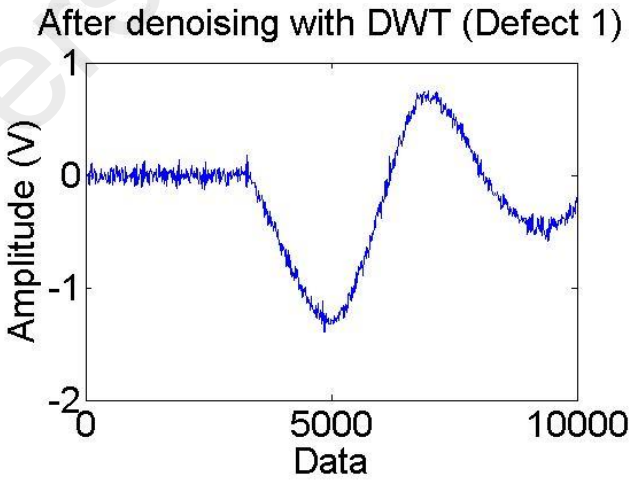


(c)

Figure 4.12: (a) Clean PD signal, (b) PD signal after adding noise and (c) denoised signal using WPT for defect C1 (insulation incision defect).

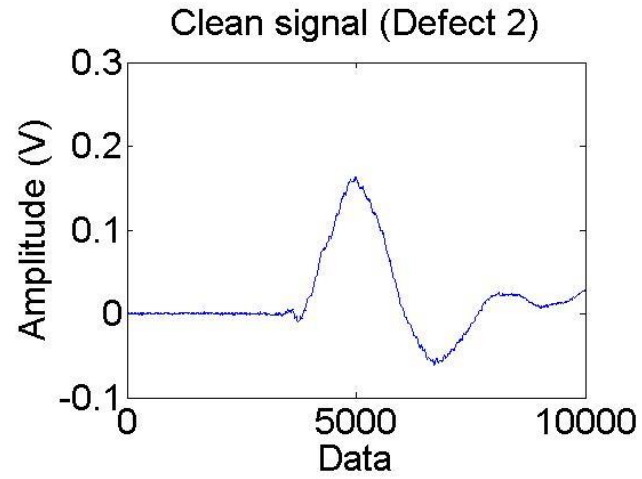


(a)

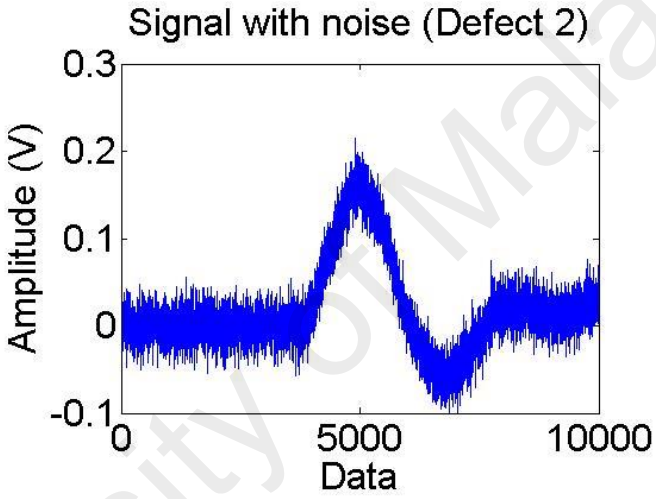


(b)

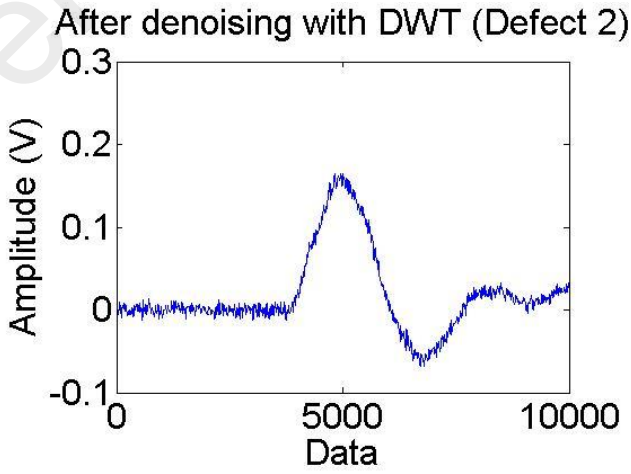


(c)

Figure 4.13: (a) Clean PD signal, (b) PD signal after adding noise and (c) denoised signal using WPT for defect C2 (axial direction shift defect).

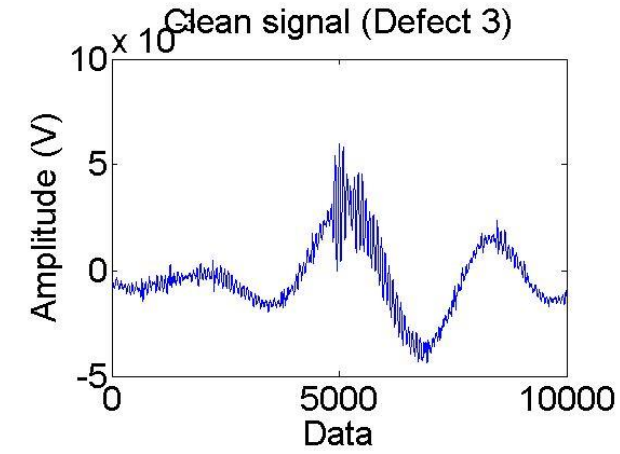


(a)

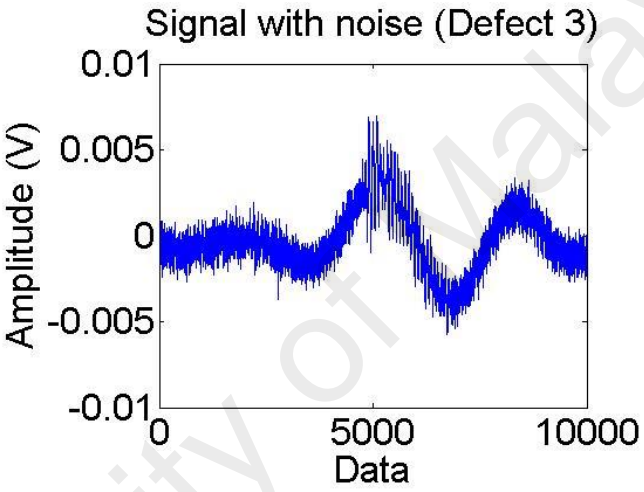


(b)

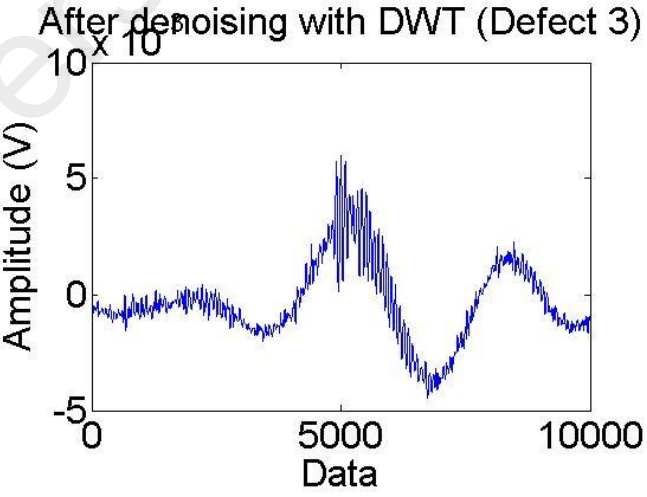


(c)

Figure 4.14: (a) Clean PD signal, (b) PD signal after adding noise and (c) denoised signal using WPT for defect C3 (semiconductor layer tip defect).

## 4.5 Comparison of accuracies among different methods

Table 4.2 shows comparison of defect determination accuracy from different denoisng methods, DFT, DWT and WPT under different signal to noise ratio (SNR) and with previous works. Each of the method was run for 10 times and the average accuracy was taken. From this table, it can be seen that DFT technique yields the highest accuracy of defect determination for cable joint defect, most accurate which is 100% at SNR =100 dB and 98.8889% at SNR = 1 dB and 10 dB. At higher SNR, the defect type determination accuracy is better for the three methods. It can also be seen that DFT-SVM yields high accuracy under different level of noise in the signals unlike DFT-ANN, which the accuracy decreases with the noise level.

Table 4.2: Comparison of defect type determination accuracies among different methods and with previous works

| **SNR** | **SNR = 1 dB** | **SNR = 10 dB** | **SNR = 100 dB** |
|---|---|---|---|
| **Method** | Accuracy (%) | Accuracy (%) | Accuracy (%) |
| **DFT-SVM** | 98.8889 | 98.8889 | 100 |
| **WPT-SVM** | 51.1111 | 55.5556 | 77.7778 |
| **DWT-SVM** | 36.6667 | 37.7778 | 71.1111 |
| **DFT-ANN [40]** | 40.0000 | 46.6667 | 100 |
| **WPT-ANN [40]** | 58.8889 | 66.6667 | 100 |
| **DWT-ANN [40]** | 56.6667 | 66.6667 | 100 |

# CHAPTER 5: CONCLUSIONS AND RECOMMENDATIONS

## 5.1 Conclusions

In this project, determination of the type of cable joint defect using partial discharge (PD) measuring equipment with added noise using support vector machine (SVM) has been successfully carried out. Five cable joints of cross-linked polyethylene type with defects introduced artificially were successfully developed according to what are commonly found at site. Various noise reduction techniques were applied to denoise the PD signals and the denoised signals were used to determine different types of defect in cable joints. The input features from different noise reduction techniques were successfully implemented to train SVM to determine the defect nature.

Determination of the defect type was successfully performed using Support Vector Machine (SVM) after DFT, WPT and DWT techniques. The results were compared between each noise reduction method and the existing work to validate the capability of the applied methods. It was found that the noise reduction technique on partial discharge signals from cable joint defects using discrete Fourier transform (DFT) yields a better accuracy than wavelet packet transform (WPT) and discrete wavelet transform (DWT). Hence, noise reduction on PD signals from cable joint defects using DFT can be a promising tool for site maintenance on cable joints.

## 5.2 Recommendations for future work

Future work that can be performed are:

1. Test using different classifiers, such as artificial neural network (ANN)
2. Test using different desnioing methods, such as Cepstrum analysis

## REFERENCES


[1] L. Niemeyer. (1995). A generalized approach to partial discharge modelling. *IEEE Transactions on Dielectrics and Electrical Insulation*, 2, 510-528.

[2] H. Mota, L.Rocha, T. Salles and F. Vasconcelos. (2011). Partial discharge signal denoising with spatially adaptive wavelet thresholding and support vector machines. *Electric Power Systems Research*, 81(2) 644-659.

[3] H. Suzuki and T. Endoh. (1992). Pattern recognition of partial discharge in XLPE cables using a neural network. *IEEE Transactions on Electrical Insulation*, 27(3), 543-549.

[4] M. Allahbakhshi and A. Akbari. (2011). A method for discriminating original pulses in online partial discharge measurement. *Measurement*, 44(1), 148-158.

[5] B. Karthikeyan, S. Gopal and M. Vimala. (2005). Conception of complex probabilistic neural network system for classification of partial discharge patterns using multifarious inputs. *Expert Systems with Applications*, 29(4), 953-963.

[6] A. Contin, G.C. Montanari and C. Ferraro. (2007). PD source recognition by Weibull processing of pulse height distributions. *IEEE Transactions on Dielectrics and Electrical Insulation*, 7(1), 48-58.

[7] H. Yu and Y.H. Song. (2003). Using improved self-organizing map for partial discharge diagnosis of large turbogenerators. *IEEE Transactions on Energy Conversion*, 18(3), 392-399.

[8] Milewski and G. Emil. (1989). The Essentials of Statistics II. *Research & Education Association*, 2.

[9] Z. Li and M. Shen. (2007). Classification of Mental Task EEG Signals Using Wavelet Packet Entropy and SVM. *8th International Conference on Electronic Measurement and Instruments*.

[10] L. Hao and P.L. Lewin. (2010). Partial discharge source discrimination using a support vector machine. *IEEE Transactions on Dielectrics and Electrical Insulation*, 17(1), 189-197.

[11] R. Sarathi, I. P. Merin Sheema and R. Abirami. (2013). Partial discharge source classification by support vector machine. *International Conference on Condition Assessment Techniques in Electrical Systems*, Kolkata, 255-258.

[12] J.K. Wong, H.A. Illias and A.H.A. Bakar. (2017). A Novel High Noise Tolerance Feature Extraction for Partial Discharge Classification in XLPE Cable Joints. *IEEE Transactions on Dielectrics and Electrical Insulation*, 24(1), 66-74.

[13] N.F.A. Aziz, L. Hao and P.L. Lewin. (2007). Analysis of Partial Discharge Measurement Data Using a Support Vector Machine. *Student Conference on Research and Development*.

[14] P.L. Lewin, J.A. Hunter, L. Hao and A. Contin (2013). Identification of PD defect typologies using a support vector machine. *IEEE Electrical Insulation Conference*.

[15] Boyle, H. Brandon (2011). Computer Science, Technology and Applications: Support Vector Machines. *Data Analysis, Machine Learning and Applications*, New York, NY, USA: Nova Science Publishers, Inc.

[16] J.K. Wong, H.A. Illias and A.H.A. Bakar. (2017). Classification of Partial Discharge Measured Under Different Levels of Noise Contamination. *Plos One*, 12(1), 1-20.

[17] M.H. Foo, J.J. Soraghan and W.H. Siew. (2005). Application of nondecimated discrete wavelet transform for partial discharge analysis. *International Conference and Exhibition on Electricity Distribution*.

[18] X. Ma, C. Zhou and I. J. Kemp. (2002). Interpretation of wavelet analysis and its application in partial discharge detection. *IEEE Trans. Dielectrics and Electrical Insulation*, 9(3), 446-457.

[19] D. Pylarinos, K. Siderakis, E. Pyrgioti, E. Thalassinakis and I. Vitellas. (2011). Impact of noise related waveforms on long term field leakage current measurements. *IEEE Transactions on Dielectrics and Electrical Insulation*, 18(1), 122-129.

[20] E.M. Lalitha and L. Satish. (2000). Wavelet analysis for classification of multi-source PD patterns. *IEEE Transactions on Dielectrics and Electrical Insulation*, 7, 40-47.

[21] D. Evagorou, A. Kyprianou, P.L. Lewin, A. Stavrou, V. Efthymiou, et al. (2010). Feature extraction of partial discharge signals using the wavelet packet transform and classification with a probabilistic neural network. *IET Science, Measurement & Technology*, 4(3), 177-192.

[22] I. Shim, J.J. Soragan, W.H. Siew, K. Sludden and P.F. Gale. (2000). Robust partial discharge measurement in MV cable networks using discrete wavelet transforms. *IEEE Power Engineering Society Winter Meeting*.

[23] G. Veloso, L.E.B. Silva, I. Noronha and G. Lambert-Torres. (2008). Identification of wavefronts in Partial Discharge acoustic signals using discrete wavelet transform. *IEEE International Symposium on Industrial Electronics*.

[24] S.G. Mallat and W.L. Hwang. (1992). Singularity detection and processing with wavelets. *IEEE Transactions on Information Theory*, 38 (2), 617-643.

[25] Brigham and E. Oran. (1988). The fast Fourier transform and its applications. *N.J.: Prentice Hall.* Englewood Cliffs.

[26] D.L. Donoho and I.M. Johnstone. (1994). Ideal spatial adaptation by wavelet shrinkage. *Biometrika*, 81 (3), 425- 455.

[27] I.J. Kemp. (1995). Partial discharge plant-monitoring technology: present and future developments. *IET Science, Measurement and Technology*, 142(1), 4-10.

[28] D.L. Donoho and I.M. Johnston. (1995). Adapting to unknown smoothness via wavelet shrinkage. *Journal of American Statistics Association*, 90 (432), 1200- 1224.

[29] B.W. Dickinson and K. Steiglitz. (1982). Eigenvectors and functions of the discrete Fourier transform. *IEEE Transactions on Acoustics, Speech and Signal Processing*, 30(1), 25–31.

[30] J.K. Wong, H.A. Illias, A.H.A. Bakar and H. Mokhlis. (2015). Partial Discharge Measurements and Classifications: Review of Recent Progress. *Measurement*, 68, 164-181.

[31] T.H. Cormen, C.E. Leiserson, R.L. Rives and C. Stein. (2001). Introduction to Algorithms, *MIT Press and McGraw-Hill* (2nd Second ed.), 822–848.

[32] G.C. Stone. (2005). Partial discharge diagnostics and electrical equipment insulation condition assessment. *IEEE Transactions on Dielectrics and Electrical Insulation*, 12(5), 891-904.

[33] Y. Tian, P.L. Lewin and A. Davies. (1995). Comparison of on-line partial discharge detection methods for HV cable joints. *IEEE Transactions on Dielectrics and Electrical Insulation*, 9(4), 604-615.

[34] Y. Tian, P.L. Lewin, P. Wang, S.J. Sutton and S.G. Swingler. (2004). Application of wavelet-based denoising to online measurement of partial discharges. *International Conference on Solid Dielectrics*.

[35] H. Zhang, T. Blackburn, B. Phung and D. Sen. (2007). A novel wavelet transform technique for on-line partial discharge measurements. 1. de-noising algorithm. *IEEE Transactions on Dielectrics and Electrical Insulation*, 14(1), 3-14.

[36] H. Zhang, T. Blackburn, B. Phung and D. Sen. (2007). A novel wavelet transform technique for on-line partial discharge measurements. 2. on-site noise rejection application. *IEEE Transactions on Dielectrics and Electrical Insulation*, 14 (1), 15-22.

[37] E. Carminati, L. Cristaldi, M. Lazzaroni and A. Monti. (2001). A neurofuzzy approach for the detection of partial discharge. *IEEE Transactions on Instrumentation and Measurement*, 50(5), 1413-1417.

[38] A.M. Atto, D. Pastor and A. Isar. (2007) Review: on the statistical decorrelation of the wavelet packet coefficients of a band-limited wide-sense stationary random process. *Signal Processing*, 87 (10), 2320-2335.

[39] A. Cavallini, G.C. Montanari, F. Puletti, A. Contin and G. Pasini. (2002). Digital detection and fuzzy classification of partial discharge signals. *IEEE Transactions on Dielectrics and Electrical Insulation*, 9(3), 335-348.

[40] H.A. Illias, G. Altamimi, N. Mokhtar and H. Arof. (2017). Classification of Multiple Partial Discharge Sources in Dielectric Insulation Material using Cepstrum Analysis-Artificial Neural Network. *IEEJ Transactions on Electrical and Electronics Engineering*, 12(3).